research articles Journal of proteome research

Chlorinated Benzenes Cause Concomitantly Oxidative Stress and Induction of Apoptotic Markers in Lung Epithelial Cells (A549) at Nonacute Toxic Concentrations

Nora Mörbt,[†] Janina Tomm,[†] Ralph Feltens,[†,‡] Iljana Mögel,[‡] Stefan Kalkhof,[†] Kalaimathi Murugesan,[†] Henry Wirth,[†,§] Carsten Vogt,[∥] Hans Binder,[§] Irina Lehmann,[‡] and Martin von Bergen*[,†,⊥]

Department of Proteomics, Department of Environmental Immunology, Department of Isotope Biogeochemistry, and Department of Metabolomics, Helmholtz Centre for Environmental Research - UFZ, Permoser Strasse 15, 04318 Leipzig, Germany, Interdisciplinary Centre for Bioinformatics of Leipzig University, D-4107 Leipzig, Haertelstrasse 16-18, Germany

Received June 8, 2010

In industrialized countries, people spend more time indoors and are therefore increasingly exposed to volatile organic compounds that are emitted at working places and from consumer products, paintings, and furniture, with chlorobenzene (CB) and 1,2-dichlorobenzene (DCB) being representatives of the halogenated arenes. To unravel the molecular effects of low concentrations typical for indoor and occupational exposure, we exposed human lung epithelial cells to CB and DCB and analyzed the effects on the proteome level by 2-D DIGE, where 860 protein spots were detected. A set of 25 and 30 proteins were found to be significantly altered due to exposure to environmentally relevant concentrations of 10^{-2} g/m^3 of CB or 10^{-3} g/m^3 of DCB (2.2 and 0.17 ppm), respectively. The most enriched pathways were cell death signaling, oxidative stress response, protein quality control, and metabolism. The involvement of oxidative stress was validated by ROS measurement. Among the regulated proteins, 28, for example, voltage-dependent anion-selective channel protein 2, PDCD6IP protein, heat shock protein beta-1, proliferating cell nuclear antigen, nucleophosmin, seryl-tRNA synthetase, prohibitin, and protein arginine *N*-methyltransferase 1, could be correlated with the molecular pathway of cell death signaling. Caspase 3 activation by cleavage was confirmed for both CB and DCB by immunoblotting. Treatment with CB or DCB also caused differential protein phosphorylation, for example, at the proteins HNRNP C1/C2, serine-threonine receptor associated protein, and transaldolase 1. Compared to previous results, where cells were exposed to styrene, for the chlorinated aromatic substances besides oxidative stress, apoptosis was found as the predominant cellular response mechanism.

Keywords: 1,2-dichlorobenzene • apoptosis • chlorobenzene • lung epithelial cells • VOC

1. Introduction

In the last fifty years, changes in lifestyle in the industrialized countries have led to prolonged times spent indoors, concurrent with the cumulative use of consumer products containing volatile organic compounds (VOCs). Therefore, many people are increasingly exposed to these chemicals which in severe cases may cause symptoms that are commonly referred to as the sick building syndrome, a condition that is characterized by irritation of the eyes, nose, throat and skin and in extreme cases even results in neuronal disorders (for review, see refs 1 and 2).

According to their structure, VOCs can be classified into aliphatic and aromatic hydrocarbons and additionally subdivided into nonhalogenated and halogenated compounds. Among the latter, chlorobenzene (CB) and dichlorobenzene (DCB) are among the most abundant representatives.[3] CB is used as an intermediate in chemical synthesis of herbicides and dyes and is also present in consumer products, such as rubber and paint.[4] In 1988, 88 500 t of DCB were produced in Western Europe.[5] Like chlorobenzene, it is mainly used as an intermediate in the chemical synthesis of pesticides but is also present as solvent in adhesives and painting material. Thus, halogenated compounds can cause severe problems since their biologically mediated degradation is rather slow and these

* To whom correspondence should be addressed. PD Dr. Martin von Bergen, UFZ Helmholtz Centre for Environmental Research, Department of Proteomics, Permoser Str. 15, 04318 Leipzig, Germany. E-mail: martin.vonbergen@ufz.de. Fax: +49-341-2351787.

[†] Department of Proteomics, Helmholtz Centre for Environmental Research - UFZ.

[‡] Department of Environmental Immunology, Helmholtz Centre for Environmental Research - UFZ.

[§] Interdisciplinary Centre for Bioinformatics of Leipzig University.

[∥] Department of Isotope Biogeochemistry, Helmholtz Centre for Environmental Research - UFZ.

[⊥] Department of Metabolomics, Helmholtz Centre for Environmental Research - UFZ.

10.1021/pr1005718

Published on Web 11/20/2010

compounds are therefore classified as persistent organic pollutants (POPs[6]).

In industry, very high occupational concentration levels have been reported for workplaces associated with the production and usage of volatile organic compounds. However, CB is not bioaccumulated to high levels and does not belong to the group of persistent organic compounds.[5,7] Only low amounts (1−9 ng/g) of CB were found in 98% of human adipose tissue samples from all regions of the United States. In addition, CB was also detected in exhaled breath, urine (20−120 ng/L), and human breast milk.[8,9]

Measured DCB concentrations in blood of the general "unexposed" population are below 3 ppb.[10] The content in whole human milk ranged from 3 to 29 ppb while 38 μg of DCB per kg fat were detected in adipose tissue.[11] Bioaccumulation is only expected in tissues with high fat content during prolonged, continuous exposures as observed in rats exposed to high concentrations of 250 mg/kg.[12]

Occupational DCB levels up to 8.5 ppm (51 mg/m^3) have been found in chlorobenzene factories.[11] For chlorobenzene, concentrations between 18.7−488 mg/m^3 were found.[13] At these high concentrations chlorobenzene can cause adverse health effects like irritation of the mucosa in nose and throat as well as headaches and dizziness.[14] In order to protect human health, German Ministry of Labor and Social Affairs (Arbeitsplatzgrenzwert, AGW) and the American Conference of Industrial Hygienists (Threshold Limit Value, TLV) adopted a limit of 10 ppm for the occupational exposure to CB. The current Permissible Exposure Limit (PEL) according to the Occupational Safety & Health Administration (OSHA) is 75 ppm. Occupational Safety & Health Administration (OSHA) adopted a Permissible Exposure Limit of 50 ppm for DCB. In 2001, the German MAK-value for DCB was lowered to 10 ppm (60 mg/m^3).[7]

Under normal circumstances, concentrations in households are too low to cause acute toxic effects. In epidemiologic studies performed in the area of Leipzig (Germany), concentrations of mono- and dichlorobenzene were found to be much lower than the reported workplace levels.[15] In particular for monochlorobenzene, concentrations in the range of 1−3.5 μg/m^3 were measured in apartments, which is comparable to those found in other studies from Germany.[16] Similar results were obtained in the United States of America.[17] While the commonly encountered indoor concentrations are not suspected to elicit acute toxic effects, epidemiological studies have shown that low VOC concentrations are correlated with an increased risk of developing atopic diseases such as eczema[15] or obstructive bronchitis.[18] Furthermore, it has been shown that low-level exposure to VOCs can also add up in affecting the developing immune system of the newborn child[19] or infants.[20] To unravel the molecular mechanisms underlying the mode of action of volatile organic compounds, the application of *in vitro* model systems is required. Since the respiratory tract is a primary site of exposure, the lung epithelial cell line A549 was selected as the model of choice for our investigations.[21] Despite the malignant nature, A549 possess typical properties of alveolar epithelial type II cells. They express multi drug resistance-associated proteins (MRP) 1 and 3 as well as most of the major constitutive and inducible CYP forms found in lung epithelial cells[22] and are able to secrete surfactant proteins, especially when cultured air-exposed.[23] Moreover, A549 cells have been shown to be competent for expressing and secreting inflammatory markers such as cytokines and chemokines in response to volatile organic compounds.[21,24]

Toxicological data for mono-, 1,2-, and 1,4-dichlorobenzene obtained in mice have indicated significant differences especially in terms of hepatotoxicity, protein droplet formation in the kidney and with respect to the serum level of thyroxine.[25] These earlier observations point to differences in the toxicological effects of the two compounds. Thus, we decided to compare these CB and DCB side by side using an *in vitro* system to study to which extent the degree of chlorination affects cellular response. Since the focus was set on nonacute effects of these two compounds, we applied a concentration range for which no significant toxicity had been observed in a previous study using chlorobenzene and the here-applied *in vitro* exposure system[26] and tested it for effects on the global proteome response.

In earlier exposure studies, the A549 cells were additionally stimulated by TNFα[24,26−28] to simulate the cells resulting in a somewhat arbitrary situation presumably resembling the *in vivo* situation of an inflammatory response occurring within the lung epithelium. However, under these conditions it is difficult to distinguish between the synergistic stimulatory effects caused by TNFα and those caused by exposure to the VOCs alone. Therefore, we decided to omit TNFα from the culturing medium in this study.

For the analysis of molecular effects, we have chosen a proteomic approach. It is a fact that a complete coverage of the cellular proteome cannot be obtained using current methods, especially regarding those proteins that are expressed in low copy numbers is not achievable. Still it is possible to use changes in the expression level or posttranscriptional modification of the more abundant proteins to gain valuable insights into the involved pathways of cellular reaction toward xenobiotic substances.[29,30] On the technical side, we opted for a 2D DIGE approach. 2D gels are not only capable to display changes in protein expression but in addition in many cases concomitantly reveal posttranscriptional modifications. Furthermore, DIGE exhibits the best sensitivity and reliability of quantification among the gel based approaches.[31] Small changes in expression are often crucial for the actual activity of proteins and thereby affect the involved molecular pathway(s) as described by the molecular species hypothesis.[32] In an earlier study we have established a reference 2D map of A549 cells[33] which proved to be helpful in this study. Although the protein expression concept has its shortcomings it has been proven to be useful in many studies in conjunction with the data evaluation following the concept of gene enrichment for identifying the most prominent processes involved. Here we are primarily interested in the cellular reaction to mono- and dichlorbenzene at nonacute toxic concentrations.

Targeted proteomic and transcriptomic approaches have shown that oxidative stress is a typical response to the VOCs monochlorobenzene and styrene.[26,34] A similar response could be identified in a global proteome approach analyzing the effects of styrene.[33] The degradation of aromatic compounds was well analyzed in earlier studies, showing that a first step catalyzed by microsomal enzymes, namely cytochrome monooxygenases, is the formation of arene epoxides, which may exert their toxic effects by forming covalent bonds with proteins and DNA.[33,35] Further transformation of the epoxides leads to the corresponding dihydrodiols and dichlorophenols.[36] Moreover, secondary metabolism of phenols may yield catechols, hydroquinones and benzoquinones. Oxidized forms of these com-

pounds together with the epoxides are supposed to be responsible for the toxicity of chlorinated benzenes.[35] The catechols were detetected in urine from all workers exposed to DCB and CB.[37,38] Moreover, secondary metabolism of phenols may yield catechols, hydroquinones and benzoquinones. Oxidized forms of these compounds together with the epoxides are supposed to be responsible for the toxicity of chlorinated benzenes.[35] The formation of catechols is caused by the activity of monooxygenases, which as a side product can also form reactive oxygen species. Furthermore, catechols themselves cause oxidative stress through the redox cycling between the quinone and the catechol with concomitant generation of damaging ROS, that in turn can cause adducts at proteins or DNA-modification.[39] Thus, the observed oxidative stress might be either a consequence of the side products from the increased activity of the monoxygenases that were induced to degrade the original chemical substance or might result directly from the formed metabolites.

However, it is still an open question to which extent aromatic VOC might drive the cells toward apoptosis. By choosing exposure conditions without obvious acute toxic effects, the dominant presence of necrotic processes can be excluded. However, proteomic changes involving components of these pathways may still occur, providing early markers for an apoptotic response developing at a later time point. The potential causative role of oxidative stress for the induction of apoptosis can be proven by the usage of antioxidative agents.[26]

The aim of this study was to detect the molecular changes in lung epithelial cells upon exposure to CB and DCB and thereby to identify the underlying molecular pathways with the final aim to define early marker proteins or sets thereof that can be used for improved precautionary testing of structurally related substances.

2. Material and Methods

2.1. Analysis of CB and DCB. CB and DCB (both Merck, Darmstadt, Germany) concentrations were measured after 24 h of exposure (10^0 g and 10^{-1} g/m^3) by automated headspace gas chromatography (GC) with a Varian 3800 gas chromatograph (Varian, Palo Alto, CA) equipped with a CP SIL 5 CB capillary column and a flame ionization detector. The chromatographic conditions as well as sample preparation and measurement were carried out in triplicates as described recently for styrene analysis.[33]

For calibrations, seven diluted standards of CB (55 μg/L−5.5 mg/L) and DCB (64.9 μg/L−6.49 mg/L) prepared from stock solutions were treated in the same way as the samples. The stock solutions were prepared in pure methanol. CB and DCB exhibited the following retention times: 2.70 and 4.44 min, respectively. The mean partition coefficients at each time point were calculated by dividing the corresponding VOC concentrations of the culture medium by the assumed VOC concentration in the atmosphere of the exposure system.

2.2. Cell Culture and Exposure to VOC. Human lung epithelial cells (A549, ATCC No. CCL-185; LGC Promochem, Wesel, Germany) were cultured (250,000 cells seeded on each transwell insert and cultivated for 3 days) and exposed in triplicates to CB (10^{-2} g/m^3) or DCB (10^{-3} g/m^3) in tightly closed prewarmed glass flasks (600 mL volume) for 24 h at 37 °C as described earlier.[21,27] Controls were exposed to methanol (VOC solvent).

2.3. Safety Measures. All operations were performed using personal protection measures defined by German law (safety glasses, gloves, and laboratory coat) as well as clean benches of the security level 2 that were additionally equipped with activated carbon filters to efficiently avoid VOC contamination of the air in the laboratory. VOC containers were stored separately in a cool place. Wastes have been collected and disposal has been managed according to German law.

2.4. Cytotoxicity Measurements. Before and after exposure, cell viability and cell numbers were recorded by Trypan blue exclusion following trypsinization of cultured cells. Membrane integrity was additionally measured using the Cytotoxicity Detection Kit (Roche Applied Science, Mannheim, Germany), according to the supplier's information. Leakage of lactate dehydrogenase (LDH) from exposed cells (triplicates) was estimated following exposure to 10^{-3}, 10^{-2}, 10^{-1}, 10^0, 10^1, 10^2 g/m^3 of CB and DCB for 24 h as published earlier for styrene. LDH release was expressed as percent of total cell LDH (determined using a lysis control).

2.5. Detection of Reactive Oxygen Species. A549 cells (500 000 cells in each well) were grown on 25 mm transwell inserts (Nunc, Roskilde, Denmark) for 24 h. Cells were washed with PBS (with Ca^{2+} and Mg^{2+}) and loaded with 25 μM 2′,7′-dichlorofluorescein diacetate (DCFH2-DA; Fluka, Seelze, Germany) for 30 min at 37 °C in the dark. After an additional wash cells were exposed to CB, DCB or methanol (control) for 2 h. Exposed cells were washed again and were harvested by incubation in 250 μL trypsin for 3 min. After resuspension in 250 μL 2% FCS-containing PBS, intracellular generation of reactive oxygen species was quantified by monitoring of fluorescence using flow cytometry (BD FACS Calibur, BD Biosciences, Heidelberg, Germany).

2.6. DIGE- 2DE. Three independent biological experiments have been performed using A549 cells exposed to CB (10^{-2} g/m^3) or DCB (10^{-3} g/m^3). For each of these experiments, cells of three transwell inserts exposed to CB or DCB in parallel in one flask were pooled as described elsewhere.[33] This has been done because of the limited cell number per transwell.

Cellular proteins of samples and controls (150 μg per sample) were precipitated with pure acetone at −20 °C for 15 min, and the precipitates were centrifuged at 20 000× *g* for 15 min. The pellets were resuspended in 30 μL of labeling buffer (30 mM TRIS pH 9.0, 7 M urea, 2 M thiourea, 4% CHAPS) as described elsewhere. Solubilisation of the precipitates was facilitated by sonication for 30 s. 2/3 of all sample volumes were then labeled using the fluorescent cyanine dyes (Cy3 for control samples, Cy5 for treated samples, 200 pmol/100 μg protein each). The remaining 50 μg of all samples were pooled for the internal standard and labeled with Cy2 (200 pmol/100 μg protein). The labeling reaction was carried out for 30 min on ice in the dark and stopped with 1 μL of 10 mM lysine per 100 μg of protein for 10 min. 100 μg of the labeled sample and control were mixed together with 100 μg of labeled internal standard to be run on one two-dimensional gel. 0.3 μL of the mixed protein solution (of each 2D-gel) were run on a 10 cm SDS-PAGE in order to verify the labeling efficiency. 340 μL of DeStreak rehydration solution containing 0.5% IPG-buffer 3−10 NL (both reagents GE Healthcare, Freiburg, Germany) were added to the remaining protein solution (∼60 μL). Samples were centrifuged at 20 000× *g* for 30 min at 20 °C. The soluble proteins in the supernatant were applied to the wells of a rehydration tray. Isoelectric focusing (18 cm IPG-strips; pH 3−10 NL) and preparations for second dimension were performed as described recently.[40] Second dimension separations (18.5 × 20 cm) were performed on PROTEAN II xi/XL system at 6 mA per

gel overnight (BIO-RAD Laboratories GmbH, Munich, Germany) until the dye front reached the bottom of the gel. During all stages of the work light exposure was carefully avoided.

2.7. Image Acquisition. Immediately after the run, DIGE gels were scanned using Ettan DIGE Image Scanner (GE Healthcare) with the following excitation/emission filters (Cy2:480 nm/530 nm; Cy3: 540 nm/595 nm; Cy5: 635 nm/680 nm). The pictures were evaluated using Image Quant software, whereby the fluorescence intensities of the most intense spot and the background were compared. The exposure time was adjusted to a value with that the most intense spot reaches the maximum of acquired gray values. After scanning, gels were stained with CBB G250 (Merck, Darmstadt, Germany) according to Neuhoff et al.[41] and dried between cellophane sheets (BIO-RAD, Munich, Germany).

2.8. Quantitative Gel Analysis. Gel pictures were quantitatively analyzed in Delta 2D version 3.6 software (Decodon GmbH, Greifswald, Germany[42]). After warping all gels (by warping the pictures of the internal standard), a fusion gel was created including all gel pictures of the experiment. Detected spots were manually edited and transferred to all gel pictures. Spot volumes (integrated staining intensity) were normalized on the total protein amount of each gel (excluding the biggest spots representing ~5% of total intensity from the normalization). Relative volumes of the spots were determined in comparison to the same spots intensity in the internal standard channel on each gel. Mean relative volumes of identical spots on triplicate gels were calculated and divided by the mean relative volume of the corresponding spots in the controls, yielding the expression ratio. Differentially expressed proteins were identified using the following parameters: expression ratio lower than 0.77 or higher than 1.3 and a p-value of $p < 0.05$, as obtained by the software's integrated Student's t test. Proteins were cut from dried gels and identified by mass spectrometry if they were significantly up- or down-regulated. Differentially expressed proteins were furthermore evaluated by multiple testing. Significantly regulated spots following multiple testing were defined by a fold change of 1.3 or higher and a tail area-based Fdr[43] < 0.1, as obtained by "fdrtool"[44] using p-values of "Delta2d's" Student's t test.

2.9. Detection of Differential Protein Phosphorylation. Differential protein phosphorylation was detected following cell exposure to CB or DCB (both at exposure to 10^0 g/m^3 and 10^{-4} g/m^3) for 1 h by Pro-Q Diamond Phosphoprotein Gel staining. Cells on three transwell inserts were washed twice with 1 mL of ice cold PBS, lyzed directly on the membranes of the inserts using 300 μL of the same lysis buffer as for the DIGE experiment, pooled in one tube and stored at −70 °C following freezing in liquid nitrogen. Experiments were performed three times including controls exposed to methanol for 1 h. Cytosol preparation and protein estimation were carried out as mentioned above. 200 μg of cellular protein were precipitated for each sample applying the described method of acetone precipitation. 135 μL of DeStreak rehydration solution containing 0.5% IPG-buffer 3−10 NL (both reagents GE Healthcare, Freiburg, Germany) were added to dried protein pellet. Samples were allowed to dissolve for 10 min under continuous shaking and they were centrifuged at 20 000× g for 30 min at 20 °C. The supernatant containing the soluble protein was applied to the wells of a rehydration tray. Proteins were focused using 7 cm IPG strips 3−10 NL (GE Healthcare, Freiburg, Germany) and prepared for second dimension as described recently.[33] Immediately after the run of the second dimension, gels were incubated in 100 mL of fixation solution (50% methanol, 10% acetic acid) for 30 min. Gels were stored in fresh fixation solution overnight at 4 °C. In the next morning gels were washed 3 times with 100 mL of doubly distilled water for 10 min and incubated (with continuous shaking) for 90 min in 50 mL of the Pro-Q Diamond Phosphoprotein Gel stain (Molecular Probes, Leiden, The Netherlands) in the dark. Afterward gels were incubated 3 times for 30 min in 100 mL of Destain solution (75% (v/v) doubly distilled water, 20% (v/v) ACN, 5% 1 M sodium acetate solution (pH 4.0)). Before gel scanning on Ettan DIGE Image Scanner (GE Healthcare), gels were rinsed twice for 10 min in doubly distilled water. Scanner settings were as following: excitation/emission filters: 540 nm/595 nm, exposure of 0.4 s per pixel. Gels were washed again in water and exposed overnight to SYPRO Ruby total protein gel stain (50 mL; BIO-RAD Laboratories GmbH, Munich, Germany). The staining solution was removed and the gels were destained for 30 min in a solution of 10% methanol and 7% acetic acid. Gels were rinsed with water and scanned using the same fluorescence scanner and the following settings: excitation/emission filters: 480 nm/595 nm, exposure of 1.0 s per pixel. Phosphostain images were quantitatively analyzed in Delta 2D version 3.6 software (Decodon GmbH, Greifswald, Germany[42]). First, all SYPRO Ruby images were warped manually and overlaid with the corresponding Pro-Q Diamond signals of the identical gels. A fusion gel (of all Pro-Q Diamond images) was created. Detected spots were manually edited and retransferred to all the Pro-Q Diamond images. Spot volumes (integrated staining intensity) were normalized on the cumulative signal on each image (excluding the biggest spots representing ~5% of total intensity from the normalization). Mean relative volumes of identical spots on triplicate gels were calculated and divided by the mean relative volume of the corresponding spots in the controls, yielding the expression ratio. Differentially expressed proteins were identified using the following parameters: expression ratio lower than 0.77 or higher than 1.3 and a p-value of $p < 0.05$, as obtained by the software's integrated Student's t test. Significantly regulated proteins were cut from wet Coomassie stained gels and identified by mass spectrometry.

2.10. Identification of Protein Spots. Tryptic digestion and protein identification using nano-HPLC-Chip/nano-ESI-ion-trap-MS or MALDI-TOF/TOF MS was carried out as described recently by Jehmlich et al.[45] In brief, the protein spots of interest were cut out of a 2D SDS-gel and digested overnight using porcine trypsin (Sigma-Aldrich, Geisenhofen, Germany). Resulting peptides were extracted from the gel, concentrated by vacuum centrifugation and analyzed either by spotting an aliquot on a MALDI stainless steel target using HCCA matrix (0.6 mg/mL) and analyzed using MALDI-TOF/TOF MS on an Ultraflex III instrument (Bruker Daltonik, Bremen, Germany) or were separated by reversed-phase nano-HPLC-Chip (LC1100 series, Agilent Technologies, Palo Alto, CA, USA; column: Zorbax 300SB-C18, 3.5 mm, 150_0.075 mm; eluent: 0.1% formic acid, 0−60% ACN) and analyzed by nano-ESI-ion trap-MS/MS (LC/MSD TRAP XCT mass spectrometer, Agilent Technologies).

For the identification of phosphorylated proteins the peptide mixtures were separated by nano-HPLC (NanoLC-Ultra 2D, Eksigent Technologies, Dublin, CA) and analyzed by an LTQ-Orbitrap hybrid mass spectrometer (LTQ-Orbitrap XL ETD, ThermoElectron, Bremen, Germany) as described by Müller et al.[46]

Database searches were performed using the MS/MS ion search (MASCOT, http://www.matrixscience.com) against all

human protein sequences of the Swiss-Prot database (http://expasy.org/sprot/). As subsequent parameters, tryptic digestion with up to one missed cleavage, carbamidomethylation of cysteines (fixed modification) and oxidation of methionines (variable modification) were used.[47] MALDI-TOF/TOF-MS data were searched with peptide mass tolerances ±100 ppm and MS/MS tolerances of ±0.6 Da. For searches of nano-HPLC-Chip/nano-ESI-ion trap-MS data peptide mass tolerances of ±1.2 Da and MS/MS fragment tolerances of ±0.6 Da were allowed, whereas peptide mass tolerances of ±10 ppm and MS/MS fragment tolerances of ±0.5 Da were used for nano-HPLC/nano-ESI-orbitrap-MS data analysis. Proteins were specified as unambiguously identified if the MOWSE score was found to be higher than 100 and at least 2 different peptides ($p < 0.05$) were used for identification. Molecular weight and p*I* of the identified protein were cross-checked with the gel position of the excised spot.

2.11. Immunoblot Analysis of Apoptosis Signaling. Ten μg of all cell lysates used for the DIGE experiment were analyzed for Caspase 3 cleavage. Protein extracts were separated using SDS-PAGE on 12% gels. Gels were electro-blotted by tank blotting on Optitran BA-S83 Reinforced Nitrocellulose (Whatman, Dassel, Germany) for 1,5 h at 100 V and 12 °C in CAPS buffer as described earlier[48] (10 mM CAPS, pH 11, 10% methanol). Protein bands were stained with Ponceau S. Membranes were incubated for 1 h in 5% skimmed milk in TBS-including 0.1% Tween 20 (TBS-T), washed three times 10 min in TBS-T and incubated overnight in the respective primary antibody dilution, containing 2% skimmed milk in TBS-T. Caspase 3-specific polyclonal rabbit antibody (#9662, Cell Signaling Technology, 1:1000) or Cleaved Caspase 3-specific polyclonal rabbit antibody (#9661, Cell Signaling Technology, 1:1000) were used for overnight incubation of membranes. After successive washing steps in TBS-T, the horseradish peroxidase-conjugated secondary antibody (goat antirabbit antibody (# 170−6515, BIO-RAD Laboratories, 1:2000) was added and incubated for 1.5 h at RT. Chemiluminescence signal was measured using Amersham ECL Advance Western Blotting detection kit (GE Healthcare, Freiburg, Germany) and FluorChem 8900 (Alpha Innotech).

2.12. Cluster Analysis of Protein Expression Data. Differential protein expression in response to CB (10^{-2} g/m^3) or DCB (10^{-3} g/m^3) as determined via 2D gel electrophoresis was compared with data obtained in a previous study,[33] where cellular effects of styrene at different concentration ($10-10^{-3}$ g/m^3) were investigated using the same experimental setup and data analysis procedure. For this, expression ratios of less than 1 (corresponding to downregulation of the respective protein) were converted to their negative reciprocals; expression ratios between the cutoff values of −1.3 and 1.3 (please see section 2.7) were set to zero. Cluster analysis of the combined data set was performed using the freely available software PAST[49] using the WARD algorithm (based on Euclidean distance), and the corresponding heatmap and dendrogram were exported. The final layout was generated using the graphic software CorelDRAW (version X3). Additionally pairwise analysis of similarities in expression changes via variance-covariance and Pearson correlation were performed for the different exposure setups (PAST). Resulting coefficients of the two analyses were combined into a single matrix (MS Excel), and from this a heatmap was generated using the freely available Java program JColorGrid.[50]

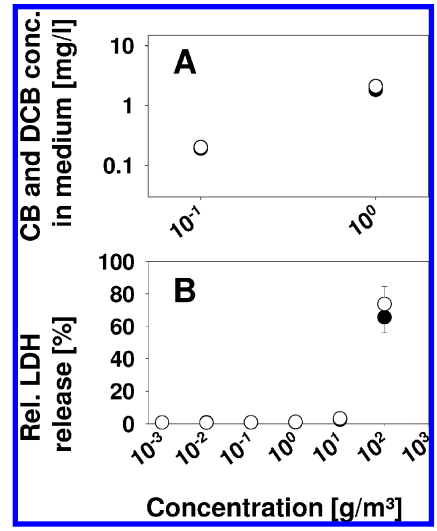

Figure 1. CB and DCB concentrations in cell culture and LDH release assessment. (A) Concentrations of CB and DCB in culture medium measured by GC in cell culture medium following A549 cell exposure to 10^{0} g and 10^{-1} g/m^3 for 24 h. (B) Toxicity of CB and DCB dichlorobenzene exposure (10^{-3} g, 10^{-2} g, 10^{-1} g, 10^{0} g, 10^{1} g and 10^{2} g/m^3 for 24 h) was measured using lactate dehydrogenase (LDH) release in A549 cells. Data are shown as mean of triplicates + SEM.

3. Results and Discussion

3.1. Cell Culture Model and Exposure of Cells to CB and DCB. In this study, transwell inserts were used for the most direct exposure of the cells to CB and DCB via the gas phase. The cells were nourished through membrane pores on the basolateral side while being exposed directly to the gas phase above them.[21,28,51] Since there is still a tiny film of medium on the cells the actual partitioning of CB and DCB between air and medium was analyzed by sampling the cell culture medium after 24 h of exposure to 10^{-1} g and 10^{0} g of both VOCs per cubic meter gas atmosphere (i.e., 19.9 and 199.0 ppm for CB; 15.23 and 152.3 ppm for DCB). This resulted in CB and DCB concentrations in the cell culture medium of 0.19 and 1.82 mg/L (1.78 μM and 18.1 μM) versus 0.20 and 2.08 mg/L (1.36 μM and 13.9 μM), respectively (Figure 1a). No CB or DCB could be detected in media of control cells which were exposed to the solvent methanol. Based on the results of the two exposure concentrations the mean partition coefficients ($c_{medium}/c_{gas\ 24\ h}$) were calculated to be 1.86 ± 0.06 for CB and 2.04 ± 0.05 for DCB. Gargas and Andersen determined a partition coefficient ($c_{0.9\%NaCl}/c_{gas}$) of 2.81 ± 0.07 for chlorobenzene[52] which is in fair accordance with our results. Further data on partitioning between cell culture medium and air are available for CB and DCB. Croute and colleagues found partition coefficients (c_{medium}/c_{gas}) of 4.66 and 3.38, respectively.[53] The higher concentration of DCB in the medium despite its reduced solubility can only be explained by its lower vapor pressure. The partition coefficients, together with the relatively small medium phase (2 mL vs 600 mL gas phase) ensured that more than 98% of the applied VOC will remain in the gas phase during the experiments and that concentrations for the gas phase thus can be calculated fairly accurately by dividing the applied amount by the total volume of the flask.

3.2. Toxicity Studies. Toxicity of CB and DCB was estimated after a 24 h exposure of human epithelial cells (A549) via the gas phase. Membrane damage was assessed (as a measure for

cell viability) by measuring cellular lactate dehydrogenase (LDH) release into the cell culture medium (Figure 1b). LDH release within 24 h increased up to 65.6% and 73.8% of total cellular LDH when cells were exposed to 10^2 g/m^3 of CB or DCB, respectively, compared to control cultures (only 0.6% of LDH_{total}). However, only a weak membrane damage of 2.41% versus 3.13% could be detected when exposing cells to 10^1 g/m^3 of CB or DCB, respectively. In a recent study on differential protein expression following 24 h styrene exposure, less severe cell membrane leakage of only 29% LDH_{total} at 10^2 g/m^3 was found. No membrane damage could be detected when cells were exposed to concentrations less than 10^1 g/m^3 of CB, DCB and styrene.[33] Thus, using this experimental readout system toxicity of the tested VOCs increases—albeit slightly—with the degree of chlorination, a result that is in line with experiments performed by Croute et al.[53] In this study, A549 cells that were exposed to 100 μM CB for 4 days showed a significant growth inhibition (−17%), whereas for the same inhibition only 10 μM of DCB were required. Even though our results do not imply such a strong dependency on the number of chlorine substituents, they give a further example of differences in toxicity between mono- and dichlorobenzenes. Since the focus of this study was to detect cellular responses upon exposition to nonacute toxic conditions, we chose concentrations that were at least 2 orders of magnitude below the lowest concentrations causing significant effects on cell viability.

3.3. Differential Protein Expression Following Exposure to CB or DCB. In this study, the effects of CB and DCB exposure on differential protein expression of lung epithelial cells (A549) were analyzed in 2D-DIGE gel triplicates. Using 10^{-2} g CB/m^3 (1.99 ppm) and 10^{-3} g DCB/m^3 (0.15 ppm), environmentally relevant concentrations were applied that are also below the governmental regulations for occupational exposure. We quantified the abundance of about 860 protein spots of A549 cells with p*I* between 4 and 9 using Delta2D software. For comparison, in a recent LC−MS based analysis of the proteomic consequences of exposure of A549 cells to H_2O_2 853 proteins were identified and quantified.[54] We identified 267 proteins in total and 50 proteins exhibited a statistical significance ($p < 0.05$) at either 10^{-2} g CB or 10^{-3} g/m^3 DCB (Figure 2A and B, Table 1), respectively. A total of 25 (for CB) versus 31 (for DCB) proteins were significantly ($p < 0.05$) regulated. Significantly regulated protein species are listed in Table 1 and a subset is displayed in more detail in Figures 2C and D and bar diagrams in Figure 3. Identification data are listed in Supplemental Table 1 (Supporting Information). We furthermore applied multiple testing to the significantly regulated spots, to confirm the significance of regulation. For CB 15 out of 25 spots (60%) and for DCB 13 out of 31 spots (42%) were found to be significantly regulated (Table 1, expression ratios marked with a filled dot) also after multiple testing.

We are aware of the shortcomings in the protein expression concept, starting with the fact that sometimes more than protein contribute to the abundance of a spot and that vice versa often different isoforms or protein species of one protein can create complicated spot pattern. We have taken care of that by checking the presence of multiple proteins in one spot by a careful look at the identification data, excluding those spots, that missed a clear difference between the first and the second hit. Furthermore the mere abundance of a protein does not necessarily imply that its activation is affected linearly. This challenge can only partially be overcome by thoroughly researching the literature on the various proteins. And finally farfetched interpretations of single proteins can be avoided by using the gene enrichment type of analysis, which requires several proteins of a process affected in order to prove its involvement and eventually testing the relevance of this process by an independent method.

Identified proteins with affected expression ($p < 0.1$) after exposure to CB or DCB are involved in different cellular processes such as cell death signaling (29), oxidative stress regulation (10), protein quality control (8) and metabolism (23). In comparison to our styrene study, where most modulated proteins were oxidative stress markers, chlorinated benzenes seem to affect predominantly cell death associated proteins

3.4. Induction of VOC Metabolizing Enzymes. The presence of aldehyde reductase (AR) was found to be doubled when exposed to 10^0 g/m^3 styrene. AR catalyzes the NADPH-dependent reduction of a wide variety of carbonyl-containing compounds to the corresponding alcohols with a broad range of catalytic efficiencies.[55] The abundance of a spot containing this enzyme was induced by 30% when cells were exposed to 10^{-3} g/m^3 of DCB thereby pointing to an increased oxidative stress-related cellular response.

Human dihydrodiol dehydrogenase isoforms are aldo-keto reductases (AKRs) that activate polycyclic aromatic hydrocarbons (PAHs) by oxidizing trans-dihydrodiol (usually produced in a primary metabolization step b phase I oxidases) carcinogens to reactive and redox-active ortho-quinones. For example, human AKR1C1 and AKR1C2 oxidize trans-7,8-dihydroxy-7,8-dihydrobenzo[a]pyrene to the cytotoxic and genotoxic metabolite benzo[a]pyrene-7,8-dione (BPQ) with the highest catalytic efficiency.[56] Two spots of AKR1C2, also called trans-1,2-dihydrobenzene-1,2-diol dehydrogenase, showed 1.85 times the normalized intensity of the same spots in the control sample following exposure to DCB. In detail, dihydrodiol dehydrogenase isoforms 1C1/2 oxidize aromatic trans-dihydrodiols to reactive and redox-active ortho-quinones which in turn cause an increased formation of reactive oxygen species (ROS) via a redox-cycling mechanism. The induction of VOC metabolizing enzymes is additionally linked to the molecular cellular event of oxidative stress because aldo-keto reductases inherently leak reactive oxygen species due to their mode of action.[57]

It is conceivable that the enzymes induction could be transmitted by the arylhydrocarbon receptor (Ahr), although the relatively small size and polar characteristics of the halides of the mono- and dichlorobenzenes confer a limited hydrophobicity and thereby allow only for a weak binding to the Ahr.[58]

3.5. Chlorinated Benzenes Modulate Oxidative Stress Proteins. Intriguingly, a number of proteins directly and directly involved in maintaining redox homeostasis were identified upon exposure to CB or DCB exposure that were recently found to be regulated also by styrene. In studies trying to explain the mechanism of toxicity of benzene[59] and halogenated benzene[60] it is argued that the oxidative attack by cytochrome P450 enzymes results in the formation of electrophilic intermediates able to react with sulfhydryl groups, leading to the depletion of reduced glutathione.[61] In order to validate the appearance of oxidative stress the effect of exposure to CB (Figure 5a,c) and DCB (Figure 5b,c) were analyzed by an intracellular assessment of reactive oxygen species. For both, CB and DCB the exposition lead to a significant increase of intracellular ROS (Figure 5c).

Increased presence (34%, $p < 0.05$) of a spot containing biliverdin reductase A (BLVRA), a potent cytoprotectant, was

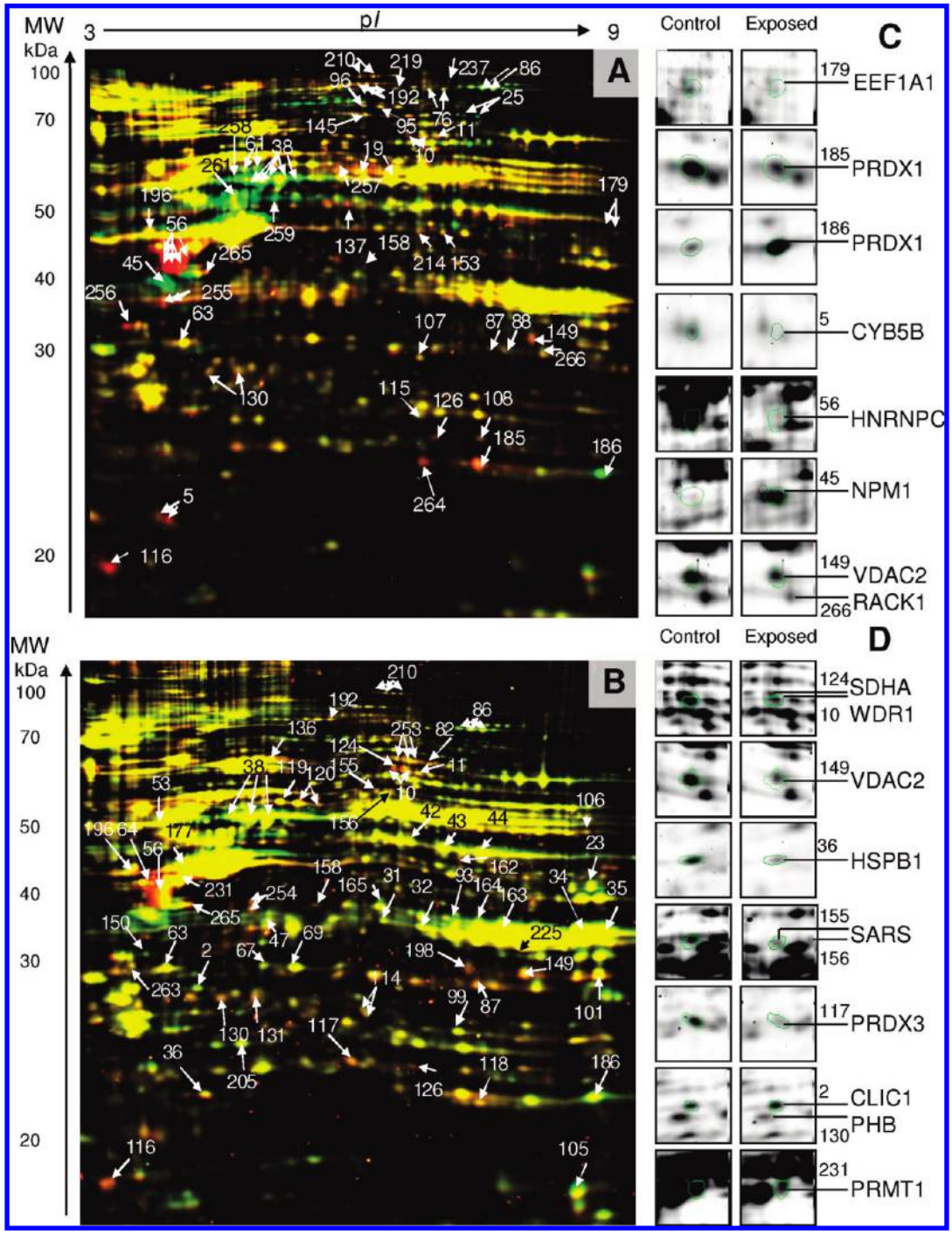

Figure 2. 2D gel electrophoresis showing differential protein expression of A549 cell line following exposure to 10^{-2} g/m^3 CB (A) or 10^{-3} g/m^3 DCB (B) compared to control cells. One-hundred micrograms of each cytosol were labeled with 200 pmol of Cy3 or Cy5 and separated on 18 cm 3−10 NL strips and 12% acrylamide gels including Cy2 labeled internal standard. Arrows mark differentially expressed protein spots with expression ratios (exposed/control) of at least >1.3 or <0.77 in triplicate experiments. Details of spot areas of differentially abundant spots are shown in C and D.

observed following DCB exposure, though to a lower extent as that observed for exposure to styrene at 10^1 g/m^3 and 10^{-3} g/m^3, respectively. Human BLVRA exerts 3% of its total activity in lung cells. Together with heme oxygenase-1, an inducible stress protein,[62,63] it converts heme via biliverding to bilirubin, the latter one being a potent antioxidant that is reverted to biliverdin upon oxidation. Thus, continuous reduction of biliverdin by BLVRA feeds a redox cycle that eliminates pro-oxidant species. The increased level of BLVRA in our experiments can be interpreted as a response mechanism to overcome VOC-induced oxidative stress.

Clic1, a redox sensitive ion channel and a member of the GST family[64] was upregulated by 50% when exposed to DCB while it reached an expression level of 250% when cells were exposed to a relatively high concentration of styrene (10^0 g/m^3). We suggest that actin-regulated membrane CLICs could modify solute transport at key stages during cellular events such as

Table 1. Differentially Expressed Proteins Following Exposure to Chlorinated Benzenes

ID[a]	protein involved in process	accession[b]	expression level[c] CB	expression level[c] 1,2 DCB
	Oxidative stress			
2	Chloride intracellular channel protein 1	O00299		1.54*
2 × 5	Cytochrome b5 type B precursor	O43169	0.27*/**/#/•	
2 × 25	Lamin-A/C	P02545	2.84°/*/#/•	
2 × 76	Glycogen phosphorylase	P11216	0.61*/#/•	
93	Aldehyde reductase	P15121		1.30*
99	Phosphoglycerate mutase 1	P18669		1.31°
162	6-phosphogluconate dehydrogenase	P52209		1.39°
164	Aldo-keto reductase family 1 member C2	P52895		1.85*/•
165	Biliverdin reductase A	P53004		1.35*
186	Peroxiredoxin-1	Q06830	2.85*	2.36°
	Cell death signaling			
2 × 10	WD repeat-containing protein 1	O75083	0.56**/•	0.49*/#/•
31	Annexin A1	P04083		1.42°
36	Heat shock protein beta-1	P04792		0.65*
6 × 38	Vimentin	P08670	3.35*/#/•	
45	Nucleophosmin	P06748	3.03*	
5 × 56	Heterogeneous nuclear ribonucleoproteins C1/C2	P07910	0.31**/***/#/•	0.39*/**/#/•
63	Annexin A5	P08758		1.59**/•
67	Annexin A4	P09525		1.31°
6 × 86	Elongation factor 2	Q8TA90	1.83°/#	1.62*/#/•
87	Electron transfer flavoprotein subunit alpha	P13804	0.60°	0.59°
95	Ezrin	P15311	0.62*/•	
101	Voltage-dependent anion-selective channel protein 1	P21796		0.61°
105	Cofilin-1	P23528		1.40°
115	Peroxiredoxin 6	P30041	0.62°	
117	Thioredoxin-dependent peroxide reductase	P30048		0.45**/•
118	Phosphatidylethanolamine-binding protein 1	P30086		0.73°
130	Prohibitin	P35232	0.60***/•	0.74*/•
149	Voltage-dependent anion-selective channel protein 2	P45880	0.57*/•	0.52***/•
150	60S ribosomal protein L5	P46777		1.48°
156	Seryl-tRNA synthetase	P49591		0.63*
158	Isocitrate dehydrogenase	Q75874	0.40*	0.31*
177	Actin, cytoplasmic 2	P63261		0.57*
2 × 179	Elongation factor 1-alpha 1	P68104	0.16*/#	0.43°/#
214	IDH1 protein	Q6FHQ6	0.65*	
219	PDCD6IP protein	Q8WUM4	0.64*	
231	Protein arginine N-methyltransferase 1	Q99873		0.33**/•
2 × 254	Actin, cytoplasmic 1	P60709		0.39*/#
256	Proliferating cell nuclear antigen	P12004	0.23°	
266	Guanine nucleot.-bind. protein subunit beta-2-like 1	P63244	0.60**	
	Protein quality control			
64	40S ribosomal protein SA	P08865		0.26*
107	Proteasome alpha 1	P25786	0.48**/•	
108	Proteasome subunit alpha type-2	P25787	0.51°	
2 × 114	Endoplasmic reticulum protein ERp29 precursor	P30040		0.70°/*/#
116	60S ribosomal protein L12	P30050	0.15*	0.38°
2 × 120	Protein disulfide-isomerase A3	P30101		0.74*/#
136	Stress-70 protein, mitochondrial	P38646		0.75*
205	Putative uncharacterized protein UCHL1	Q4W5K6		1.79*
	Metabolism			
2 × 19	Retinal dehydrogenase 1	P00352	0.59°/#	
23	Phosphoglycerate kinase 1	P00558		1.73°
34	Glyceraldehyde-3-phosphate dehydrogenase	P04406		1.54°
43	Alpha-enolase	P06733		1.68**/#
2 × 53	Tubulin beta chain	P07437		1.40**/•
2 × 61	Keratin, type II cytoskeletal 7	P08729	1.51*	
82	ATP-dependent DNA helicase 2 subunit 1	P12956		0.57**/•
106	ATP synthase subunit alpha, mitochondrial	P25705		0.65°
124	Succinate dehydrogenase flavoprotein	P31040		0.51*/•
126	Heterogeneous nuclear ribonucleoprotein H	P31943	0.37*	0.48°
137	Eukaryotic initiation factor 4A-III	P38919	0.62°	

Table 1. Continued

ID[a]	protein involved in process	accession[b]	expression level[c] CB	expression level[c] 1,2 DCB
145	Glycyl-tRNA synthetase	P41250	0.63*/•	
153	Elongation factor Tu	P49411	0.66*/•	
5 × 192	Neutral alpha-glucosidase AB	Q14697	0.49*/**/#/•	0.72°
196	Reticulocalbin 1 precursor	Q15293	0.52°	0.54*
198	Thiosulfate sulfurtransferase	Q16762		0.54*
4 × 210	Carbamoylphosphate synthetase I	Q5R208	0.53***/***/#/•	0.57*/*/#
225	Annexin A2	Q8TBV2		1.75°
237	2-Oxoglutarate dehydrogenase E1 component	Q9UDX0	0.39°	
3 × 253	Moesin	P26038		0.69*/*/#
3 × 255	Elongation factor 1-delta	P29692	0.48°/**/#/•	
2 × 258	G-rich sequence factor 1	Q12849	0.56°/°/•	
263	Tropomyosin alpha-1	P09493		0.71*

[a] For spot IDs see map in Figure 2. [b] Uni-Prot Accession from www.uniprot.org. [c] Expression level (exposed versus control)) following exposure to monochlorobenzene (10^{-2} g/m^3) or 1,2 dichlorobenzene (10^{-3} g/m^3. ° $p < 0.1$, * $p < 0.05$, ** $p < 0.01$, *** $p < 0.001$. Mass spectrometric identification data are found in the supplemental Table 1 (Supporting Information). # median value was calculated out of at minimum two values for those the significance level is indicated separately. • protein spots significantly regulated following multiple testing (with an fold change in expression >1.3 and a tail area-based Fdr <0.1, as obtained by "fdrtool" using p-values of "Delta2D"s Student's *t* test. # median value was • protein

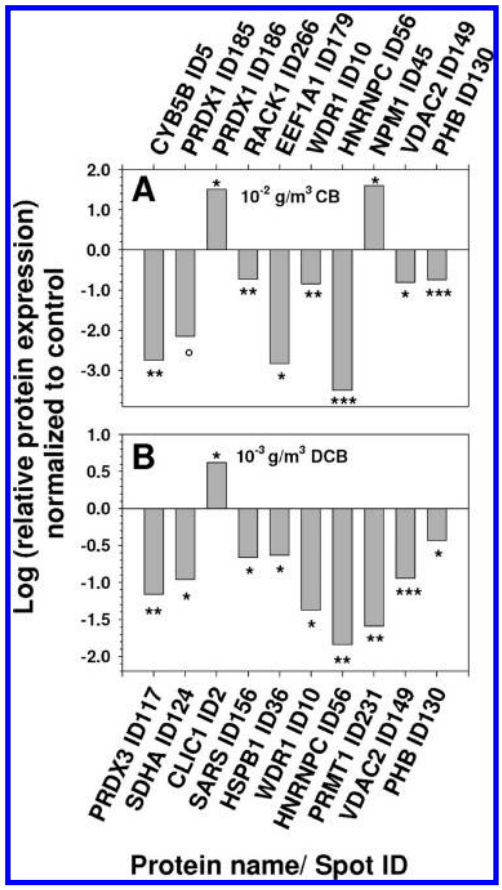

Figure 3. Statistical summary of differentially expressed proteins following exposure to (A) 10^{-2}g/m^3 CB or (B) 10^{-3}g/m^3 DCB. Expression levels are spot volumes relative to spot volumes of control calculated as means of 3 replicates. Abbreviations are gene names. ID numbers are listed in table 1 and Supplemental Table 1 (Supporting Information).

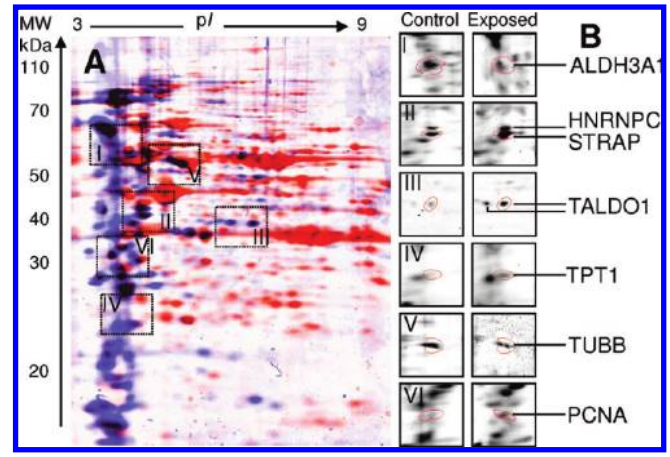

Figure 4. 2-DE phosphoproteome analysis of 200 μg of A549 cell lysates following exposure to CB and DCB. (A) Overlay of the phosphoprotein-specific signal (Pro-Q Diamond, Molecular Probes, in violett) compared to the total protein (stained with SYPRO Ruby, in red). (B) Details as enlarged gel image regions of differentially expressed proteins from triplicate experiments with 10^0 g or 10^{-4} g/m^3 of CB and DCB. Enlarged regions are marked with dotted squares in A. Protein expression and identification data are listed in Supplemental Table 2 (Supporting Information).

apoptosis, cell and organelle division and fusion, cell-volume regulation, and cell movement.

A key enzyme of the pentose phosphate pathway (PPP) was found to be affected by the exposing A549 cells with styrene. Synthesis of reduced glutathione from the oxidized form is completely dependent on NADPH produced by the PPP.[65,66] Here, 6-phosphogluconate dehydrogenase (PGD), which is also involved in NADPH synthesis, was significantly up-regulated by more than a factor of 2 when exposed to 10^0 g/m^3 styrene. In cells exposed to 10^1 g/m^3 of styrene (+80%) and 10^{-3} g/m^3 of DCB (+39%), the spot was detected with increased intensity compared to control cells but with lower significance ($p < 0.1$). Kozar et al. observed stimulation of the PPP including PGD during the recovery period from acute lung injury and concluded that both the PPP and the GSH system contribute to the recovery phase of oxidant-mediated lung injury.[67]

Isoforms of peroxiredoxin, for example, peroxiredoxin 3 are involved in oxidative stress response as well as apoptosis. Being a negative regulator of apoptosis, the protein becomes oxidized at the onset of apoptosis, which occurs within the same time frame as increased mitochondrial oxidant production, caspase activation and cytochrome c release. A 63% decrease of the intensity of one spot which was identified as peroxiredoxin 6 was observed following CB exposure. However, it cannot be

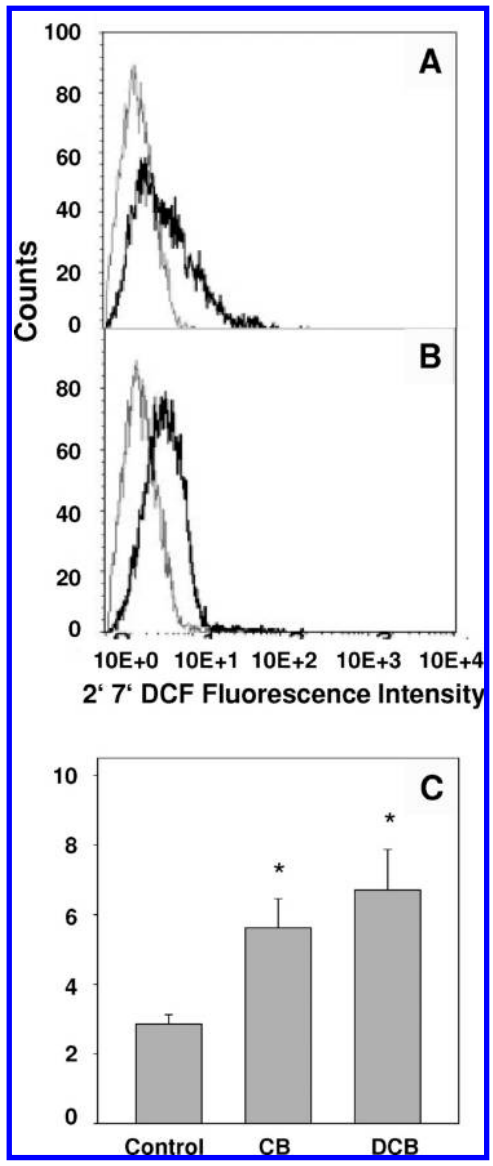

Figure 5. Detection of intracellular reactive oxygen species. ROS were detected by 2′7′ DCF fluorescence after exposure to VOC (A) 10^{-2} g/m^3 CB or (B) 10^{-3} g/m^3 DCB. Control samples are shown in gray, samples as black lines. (C) FACS staining is summarized and significant differences ($p < 0.05$) between samples and controls are indicated by asterisk.

deduced if this indicates a potential change in the rate of synthesis or degradation of the protein, since the spot may also merely represent a modified or degraded species of peroxiredoxin 6. In line with our observations, a study investigating age related cataracts found that epithelial cells with targeted inactivation of peroxiredoxin 6 expression showed higher ROS expression and were prone to apoptosis.[68]

Oxidative stress is linked to further signaling pathways, most prominently with the NF-κB and the p38 MAPK pathways, which both can also trigger apoptosis. Evidence for a connection of exposure to VOCs and the NF-κB pathway is also provided by studies in which the induction of the NF-κB and the p38 MAP kinase pathway via a redox-specific mechanism was shown in response to chlorobenzene[24,26] or styrene[28]

3.6. Chlorinated Benzenes Affect the Abundance of Cell Death-Related Proteins. A large number of proteins with differential abundance were found that are involved in apoptotic pathways. Therefore, we confirmed the extent of apoptosis by analysis of the apoptosis marker caspase 3 in CB and DCB treated cell lysates (Figure 6). Treatment of cells with CB and DCB induced cleavage of caspase 3 resulting in the 17 kDa active fragment.

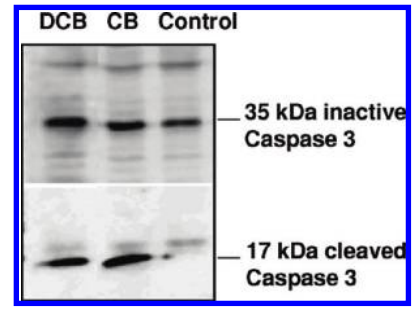

Figure 6. VOC exposure increases Caspase 3 cleave. Ten micrograms of cytosolic protein from the identical samples as were used for DIGE experiments (exposure to 10^{-2} g/m^3 CB or 10^{-3} g/m^3 DCB) were applied to standard Western blot analysis using Caspase 3-specific polyclonal rabbit antibody (#9662, Cell Signaling Technology, 1:1000) or cleaved (active) Caspase 3-specific polyclonal rabbit antibody (#9661, Cell Signaling Technology, 1:1000). One experiment out of three is shown.

In terms of proapoptotic regulation the proteins hnRNPC1/C2, VDAC2, WDR1/Aip1, prohibitin were found to be regulated. A cluster of spots containing heterogeneous nuclear ribonucleoproteins C1/C2 (hnRNPC1/C2) showed a strong downregulation to a remaining level of only 8.8% for CB ($p < 0.001$) vs 21.6% for DCB relative to the expression in control cells. Holcik reported that cellular hnRNPC1 and -C2 levels correlate positively with the XIAP (X-linked inhibitor of apoptosis) IRES (internal ribosome entry site) activity *in vivo*.[69] XIAP is the most powerful and ubiquitous intrinsic inhibitor of apoptosis by virtue of blocking caspase activation. In this study, reduced levels of hnRNPC were observed supporting the hypthesis that hnRNPC1 and -C2 bind to the XIAP IRES element and are thus involved in the modulation of XIAP IRES translation. It was supposed that the proteolytic cleavage of hnRNPC1 and -C2 at the onset of apoptosis could be targeted to attenuate the synthesis of the antiapoptotic molecule XIAP.

Voltage dependent anion channel 2 (VDAC2) showed a more than 40% decreased abundance when exposed to both of the chlorinated compounds ($p < 0.05$ for CB; $p < 0.001$ for DCB). This mitochondrial outer-membrane protein, that was also significantly decreased when cells were exposed to a wide range of styrene concentrations, interacts specifically with the inactive conformer of the multidomain pro-apoptotic molecule BAK. Reduced levels of VDAC2 make cells more susceptible to apoptotic death.[70] Two spots of WD-repeat-containing protein 1 (WDR1/Aip1) were observed to be significantly reduced (to a level of 56% ($p < 0.01$) vs 39% ($p < 0.05$), respectively) in abundance following cell exposure to CB or DCB. Extensive investigations have indicated that WDR1 is linked to apoptotic actin depolymerization by binding a cofilin/actin complex, and enhancing cofilin's capacity to sever actin filaments.[71] Additionally, caspase 3 is known to cleave the actin filament severing protein gelsolin; the resulting fragment then cleaves actin and in turn leads to morphologic changes in apoptotic epithelial cells.[72] Indeed, actin 1 abundance seemed to be downregulated to a level of 36% by CB, whereas actin showed almost 58% compared to controls when exposed to DCB. A linkage between oxidative stress, VDAC and actin depolymer-

ization was proposed by Gourlay et al. as they report on a direct coupling of ROS release to actin function caused by opening and closing of the VDACs, mitochondrial membrane pores regulating the release of proapoptotic factors such as cytochrome c. In purified mitochondria from *N. crassa*, addition of an actin-stabilizing drug, phalloidin caused prolonged opening of VDAC pores and an increase in released ROS, suggesting that actin has a conserved role in cell death by regulating VDAC in eukaryotic cells.[73]

Prohibitin displayed a reduction in abundance of about 40% for CB and 35% for 1,2-DCB ($p < 0.001$ for CB; $p < 0.01$ for 1,2-DCB). Fusaro and co-workers presented prohibitin as a potential tumor suppressor protein that can repress activity of the E2F transcriptions factors. Especially E2F1 is known for its ability to induce apoptosis (reviewed in[74]); this is achieved through induction of pro-apoptotic genes, including Apaf-1 and p73. Prohibitin was found to bind to the pocket domain of Rb family members and contact E2F family members through the marked box domain.[75] Prohibitin has been shown to inhibit apoptosis in at least two different scenarios: in camptothecin-induced apoptosis as well as growth factor withdrawal-induced apoptosis.[76] Hence, reduced prohibitin levels following exposure to chlorinated VOCs may indicate induced cell death signaling.

The nucleophosmin (NPM) protein spot showed more than three times abundance compared to control level while cellular exposure to CB ($p < 0.05$). NPM is a multifunctional protein that plays important roles in the regulation of cell proliferation and apoptosis.[77] Induction of NPM protein expression was described in human lung non small cell carcinoma cell line H460 treated with different apoptosis-inducing agents.[78]

Heat shock protein B1 (HSPB1) expression was decreased to a level of about 64% (relative to the control) at 10^{-3} g/m^3 of 1,2-DCB ($p < 0.05$). Recently we showed that after cellular exposure to styrene HSPB1 was also significantly reduced in abundance.[33] HSPB1 is known for its role in apoptosis signaling.[79] Pandey and colleagues demonstrated that HSPB1 inhibits cytochrome c-dependent activation of caspase 3. In their experimental setup, HSPB1 associated with Caspase 3, but not Apaf-1 or Caspase 9, and inhibited activation of Caspase 3.[80] Additionally, it has been shown previously that HSPB1 down-regulation results in induction of NF-kappa B (NF-κB) reporter activity and increases the release of the pro-inflammatory cytokine IL-8 in human keratinocytes.[81] Further, HSPB1 siRNA increases basal and tumor necrosis factor alpha-mediated activation of NF-κB pathway in HeLa cells.[82]

60S ribosomal protein L5 (RPL5) was up-regulated with lower significance ($p < 0.1$) when cells were exposed to 10^{-3} g DCB/m^3. This protein was significantly up-regulated when cells were exposed to styrene. RPL5 was recently identified as a substrate of death-associated protein kinase (DAPk), a serine/threonine kinase whose contribution to cell death is well established.[83]

Casas and colleagues provided evidence that seryl-tRNA synthetase is a substrate of caspase 3 *in vitro*.[84] We suppose that the more than 35% lowered abundance ($p < 0.05$) of two protein spots identified as seryl-tRNA synthetase could be caused by cleavage by activated caspase 3.

Another sign of VOC mediated apoptosis induction is the 40% decrease ($p < 0.01$) in spot intensity of guanine nucleotide-binding protein subunit beta-2-like 1, also called receptor of activated protein kinase C 1 (RACK1), following cellular exposure to CB. RACK1 is a 36-kDa cytosolic protein, which belongs to the WD-40 family of proteins, characterized by highly conserved, internal WD-40 repeats (Trp-Asp) implicated in protein−protein interactions, and is a homologue of the beta subunit of G-proteins. RACK1 shows specific binding to the active form of PKC beta isoforms, and interaction with several other important signaling proteins, for example, the Src kinase family.[85] Overexpression of full-length RACK1 in T cell lines resulted in resistance to dexamethasone- and ultraviolet-induced apoptosis. Down-regulation of RACK1 using RNA interference abolished the resistance of the transfected cells to apoptosis. Together, these findings suggest that RACK1 plays an important role in the intracellular signaling pathways that lead to apoptosis.[85]

Recently, Tuck et al. observed airway epithelial cell apoptosis in the acute injury phase after Cl_2 exposure (≤24 h postexposure, 800 ppm for 5 min). In the repair phase after Cl_2 exposure increased airway epithelial cell proliferation, measured by immunoreactive proliferating cell nuclear antigen (PCNA) was recognized. Here, the much lower proliferation rate of only 23% compared to untreated cells while cells are stressed by CB and undergo cell death was expected from literature.[86]

Other proteins that are known to accompany or facilitate increased apoptosis as annexin A1 and protein arginine *N*-methyltransferase 1 were found to be upregulated and thereby allowed an increased apoptosis. Annexin A1 is known for its anti-inflammatory function, its involvement in the ERK repression pathway and apoptosis.[87] We found a more than 50% increased abundance of a spot containing annexin A1 when cells were exposed to DCB as well as to styrene. Annexin A1 was also proposed as a stress protein in A549 cells.[88]

We observed significant ($p < 0.01$) repression of protein arginine *N*-methyltransferase 1 (PRMT1) to a level of 33% versus controls following exposure to DCB. PRMT1 was identified as coactivator of p53 involved in the methylation of histones H3 and H4 to facilitate p53-mediated transcription. The induction of apoptosis was also proven by the cleaved fragment of Caspase 3 which is significantly increased after exposure to CB and DCB (Figure 6).

In conclusion, there is substantial evidence that a large proportion of the differentially regulated proteins act in favor of apoptosis by increasing apoptotic activity.

3.7. Metabolic Changes. Around 30% (23 proteins) of the proteins differentially regulated following CB or DCB exposure can be connected to cellular metabolism in the widest sense, namely ribosomal proteins as well as proteins such as GARS protein and glycogen phosphorylase. Several authors emphasized the interrelation of oxidative stress with metabolic changes, although it remains challenging to explain the mechanism behind[89,90] this conjunction.

3.8. Chlorinated Benzenes Modulate Protein Phosphorylation. The combination of 2-D gel electrophoresis and modification specific staining of phosphorus moieties with Pro-Q Diamond offers the qualitative and also quantitative detection of phosphorylated serine and threonine residues and has been used successfully especially for the analysis of proteomic changes induced by oxidative stress.[91] In a study by Orsatti, the fluorescence signal was plotted against the moles of protein and showed linearity over 3 orders of magnitude for each protein. The slope of the line for each protein was then plotted against the known number of phosphates per protein, showing a strong correlation between the two parameters.[92]

In this study (Figure 4) 18 significantly altered proteins were identified (see also Supplemental Table 2, Supporting Information). All identified proteins are well-known phosphoproteins

(listed as such in UniProtKB/TrEMBL database) or have predicted phosphorylation sites (in PhosphoSitePlus; www.phosphosite.org). Due to the bias of DIGE for proteins of intermediate to higher abundance, it is unlikely to detect signaling molecules such as kinases but phosphorylation does also alter activity or interaction of metabolizing proteins.

Transaldolase (TALDO1) showed a more than doubled abundance as a phosphorylated protein at the concentration of 10^{-1} g/m^3 CB. Spot intensity was increased to a lesser extent at lower exposure concentrations. TALDO1 acts as key enzyme of the nonoxidative branch of the PPP. Banki et al. proposed that GSH levels and sensitivity to apoptosis are regulated by changes in TALDO1 expression in human cells.[93]

Lachaise and colleagues suggested that regulation of transaldolase activity is achieved by posttranslational modification of the protein. The researchers identified a complex set of transaldolase isoforms and postulated that changes in the phosphorylation of specific isoforms could be correlated with the different enzymatic activities seen.[94]

The phosphorylation of one isoform of the heterogeneous nuclear ribonucleoprotein C1/C2, which is involved in the early steps of spliceosome assembly and pre-mRNA splicing, was found to be increased by more than 2-fold in cells incubated with 10^{-1} g/m^3 CB. Interestingly, a decrease in spot intensity of the same protein was detected in the DIGE approach, raising the possibility that for this protein the observed change does not reflect a shift in protein amount but instead indicates a corresponding difference in post translational modification of this isoform. For hnRNP there are 14 known phosphorylation sites reported, so it remains uncertain, which specific type of phosphorylation was observed here. As hnRNP interacts with the 3′-UTR or 5′-UTR of mRNA, modulating the stability and the level of translation of bound mRNA molecules,[95] its phosphorylation status is of major interest, as it most likely plays a key function in the functionality of the protein.[96]

The alpha-enolase, a multifunctional enzyme that, despite its role in glycolysis, plays a part in various processes such as growth control, hypoxia tolerance and allergic responses, was also found to be phosphorylated.[97]

As third protein, the serine-threonine kinase receptor-associated protein (STRAP), is one of the important proteins regulated by phosphorylation.[98] Due to phosphorylation the STRAP inhibits ASK-1 (apoptosis signal regulating kinase1) mediated signaling to both JNK and p38 kinases by stabilizing complex formation between ASK1 and its negative regulators.

Moreover, quantification of protein phosphorylation with Pro Q Diamond revealed a significantly enhanced phosphorylation of HNRPC1/2 following cell exposure to low and high CB concentrations. Recently, Kyle et al. identified a previously unknown regulatory cis-element within the coding region of p53 mRNA, which interacts with HNRNPC1/C2, and pointed out that this interaction is critical for the activation of p53 finally leading to apoptosis. They showed that HNRNPC1/2 bind strongly and specifically, in a phosphorylation-dependent manner, at this site in response to DNA damage and inhibition of transcription.[99] Phosphorylation on Ser-260 and Ser-299 occurs typically in resting cells, while phosphorylation on Ser-253 and on one serine residue in the poly-Ser stretch at position 238 is a known response to hydrogen peroxide stress.[100]

Overall, 14 possible HNRPC1/2 phosphorylation sites (serine) are listed in the UniProtKB/TrEMBL database, which amounts to a theoretical number of 2^{14}= 16 384 differentially phosphorylated isoforms. However, as isoelectric focusing can only resolve isoforms with different numbers of phosphate residues, but cannot discriminate between phosphorylation at different sites, a maximum of 14 or 15 different protein species is principally detectable using the two-dimensional Pro Q Diamond or DIGE approaches, respectively. Furthermore, since protein kinases are known to often phosphorylate more than one residue of their respective targets, certain phosphorylation patterns may simply not occur in detectable amounts within a biological context. And even if all of the postulated sites indeed represented actual phosphorylation sites, different isoforms would have been identified only if their relative amounts had been affected by our exposure experiments.

In conclusion, also the changes in phosphorylation hint to oxidative stress and apoptosis as the early molecular response of the cells in this model which is in concordance with epidemiological data that could associate VOC burden with biomarkers of oxidative stress in the urine of patients.[101]

3.9. Marker Sets for the Cellular Reaction toward Aromatic and Halogenated Aromatic Compounds. Using existing data sets on proteomic changes in lung epithelial cells upon exposure to the aromatic compound styrene[33] and the data set for exposure to halogenated aromatic compounds at subacute concentrations obtained in this study, a comparison can be made to identify common effects and differences (see Figure 7a). In terms of commonly affected proteins, surprisingly there were only two proteins, namely the voltage-dependent anion-selective channel protein 2 and peroxiredoxin-1 that were changed in the same manner over all exposures. Both proteins belong to the molecular pathways that were most prominent in our studies, the oxidative stress response and apoptosis.

The differential abundance of proteins was plotted as a heatmap displaying all proteins that were up- or down-regulated by at least 30% (Supplemental Figure 1, Supporting Information). Regarding the cluster of proteins affected by styrene exposure, it is obvious that there is a general trend toward changes becoming more pronounced and numerous with increasing styrene concentrations. Another aspect is the clear difference between the expression pattern changes of the halogenated aromatic substances when compared to styrene-induced patterns.

For a more detailed analysis of the similarity of regulated protein patterns between the different exposure schemes, correlation (Pearson) and covariance coefficients were calculated and results presented in the form of a heatmap (Figure 7b). Though the two different types of coefficient do not cover the same range of values, the table has an overall symmetrical appearance. Data from the CB experiments show nearly no similarity to styrene data (correlation and covariation values below 0.2) but is somewhat similar to the DCB data set in terms of Pearson correlation and higher similar in terms of covariance. Likewise, DCB-induced expression patterns are similar to CB, but also show a modest correlation and covariance to the pattern obtained with the highest styrene concentration. This makes sense, since the effects of oxidative stress and also apoptosis were found to be of increased significance at higher concentrations of styrene.[33] This finding is consistent with the assumption that the oxidative stress caused by styrene is concentration dependent and that DCB has a higher toxicological potential as it is reflected in the lower concentration needed to cause detectable toxicological effects.

The two halogenated substances cause common changes beside the two ubiquitously regulated proteins in a total of 10

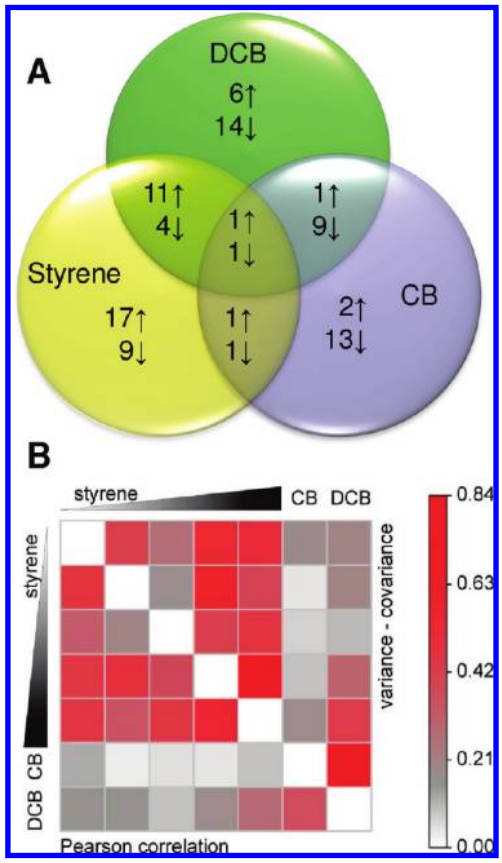

Figure 7. Overlap and similarity between effects on proteome level after exposure to CB, DCB and styrene. Expression data following styrene exposure were recently published[33] and only those proteins were taken into account for the (A) Venn diagramm that showed regulation in the same direction. For the analysis of similarity between pattern of changes pairwise Pearson correlation and covariance coefficients were calculated using all proteins showing an expression change of at least 1.3-fold and are represented below and above the white diagonal of the heatmap, respectively.

proteins, whereas the overlap between styrene (all concentrations combined) and both CB and DCB accounts for 17 proteins. More importantly, there are significant differences between the sets of overlapping proteins in respect to their molecular functions. Among the proteins commonly altered in abundance in presence of halogenated aromatic compounds there are proteins correlated with apoptosis like WD repeat-containing protein 1 and the heterogeneous nuclear ribonucleoproteins C1/C2 and the elongation factor 1 alpha 1 as an indicator for general decrease of cell vitality.

The least common features are shared by CB and styrene, among those two experiments only 2 proteins were found to be regulated in the same manner, namely glycogen phosphorylase and vimentin. Whereas the proapoptotic ezrin and the Hnrph1 are upregulated in styrene they were found to be downregulated in response to CB pointing to different pathways leading to apoptosis and different stages at the time point of sampling in CB in comparison to styrene.[102]

Although oxidative stress is a common feature in all exposure scenarios, there are different proteins indicated here, for the styrene-type of altered protein expression peroxiredoxin-4 and DJ-1 were found exclusively whereas the biliverdin reductase A was affected by styrene and DCB but not by CB. These results point to a more complex pattern in the generation of oxidative stress depending on the various VOCs and hold the promise that specific stages of oxidative stress can be defined as shown also for the effect of diesel exhaust by Xiao et al.[103]

The same might hold true for the induction of detoxification, since in the case of DCB the aldo-keto reductase family 1 member C2 was affected that was correlated with the xenobiotic response toward lipid peroxidation byproduct in mice.[104] For the halogenated compounds the retinal dehydrogenase (in the case of chlorobenzene and styrene) was found and it is reported to be coregulated with CYP450,[105] the aldehyde dehydrogenase 3A1 (after exposure to styrene and DCB) was reported to be regulated by xenobiotic response controlled by arylhydrocarbon receptor.[106]

4. Concluding Remarks

The detection of specific molecular effects oton the proteome as a measure for the cellular response toward volatile organic compounds sheds light on the activity of those compounds that are present indoors and thereby constitute a risk for human health. The observed effects of induced oxidative stress response and apoptosis caused by concentrations below current occupational limitations and 2 orders of magnitude below any acute toxic effects underline the concern about the presence of volatile organic compounds. The comparison of effects observed for different classes of VOCs will allow deciphering the different modes of action and will reveal protein marker patterns that in turn will help to characterize the possible effects of structurally related new compounds before they are released into the human environment.

Abbreviations: CB, monochlorobenzene; DCB, 1,2-dichlorobenzene; VOC, volatile organic compound; 2D, two-dimensional; DIGE, fluorescence difference gel electrophoresis.

Acknowledgment. We thank Yvonne Kullnick, Franziska Kohse, Michaela Öhler, and Kerstin Krist for cooperation and technical assistance and Carmen Röder-Stolinski for methodological support and helpful discussions.

Supporting Information Available: Supplemental tables and figure. This material is available free of charge via the Internet at http://pubs.acs.org.

References

(1) Hodgson, M.; Levin, H.; Wolkoff, P. Volatile organic compounds and indoor air. *J. Allergy Clin. Immunol.* **1994**, *94* (2 Pt 2), 296–303.
(2) Molhave, L. Indoor climate, air pollution, and human comfort. *J. Expo. Anal. Environ. Epidemiol.* **1991**, *1* (1), 63–81.
(3) Rehwagen, M.; Schlink, U.; Herbarth, O. Seasonal cycle of VOCs in apartments. *Indoor Air* **2003**, *13* (3), 283–91.
(4) Willhite, C. C.; Book, S. A. Toxicology update. *J. Appl. Toxicol.* **1990**, *10* (4), 307–10.
(5) Heinisch, R. J.; Kettrup, A.; Bergheim, W.; Martens, D.; Wenzel, S. Persistent chlorinated hydrocarbons (PCHC), source-orientated monitoring in aquatic media. 4. The Chlorobenzenes. *Freesenius Environ. Bull.* **2006**, *15* (3), .
(6) Boethling, R.; Fenner, K.; Howard, P.; Klecka, G.; Madsen, T.; Snape, J. R.; Whelan, M. J. Environmental persistence of organic pollutants: guidance for development and review of POP risk profiles. *Integr. Environ. Assess Manag.* **2009**, *5* (4), 539–56.
(7) CDC, NIOH and NIOSH basis for an occupational health standard: chlorobenzene MMWR Morb Mortal Wkly Rep 1994, *4*, (43, 148−149).
(8) ATDSDR, Toxicological profile for chlorobenzene. Agency for Toxic Substances and Disease Registry (ATDSR), 1990.
(9) ATSDR, Toxicological profile for chlorobenzene. Agency for Toxic Substances and Disease Registry (ATDSR), 1990.

(10) ATSDR, Toxicological profile for Dichlorobenzene. Agency for Toxic Substances and Disease Registry (ATDSR), 2006.
(11) Howard, P. Large Production and Priority Pollutants. *Handbook of Environmental Fate and Exposure Data for Organic Chemicals*; Lewis Publishers: 1989.
(12) Hissing, A. M.; Van Ommen, B.; Van Bladeren, P. J. Dose dependent kinetics and metabolism of 1,2-dichlorobenzene in rat; effect of pretreatment with phenobarbital. *Xenobiotica* **1996**, *26* (1), 89–105.
(13) Kusters, E.; Lauwerys, R. Biological monitoring of exposure to monochlorobenzene. *Int. Arch. Occup. Environ. Health* **1990**, *62* (4), 329–31.
(14) von Burg, R. Toxicology updates. Monochlorobenzene. *J. Appl. Physiol.* **1981**, *95* (6), 2444–52.
(15) Diez, U.; Kroessner, T.; Rehwagen, M.; Richter, M.; Wetzig, H.; Schulz, R.; Borte, M.; Metzner, G.; Krumbiegel, P.; Herbarth, O. Effects of indoor painting and smoking on airway symptoms in atopy risk children in the first year of life results of the LARS-study. Leipzig Allergy High-Risk Children Study. *Int. J. Hyg. Environ. Health* **2000**, *203* (1), 23–8.
(16) Hippelein, M. Background concentrations of individual and total volatile organic compounds in residential indoor air of Schleswig-Holstein, Germany. *J. Environ. Monit.* **2004**, *6* (9), 745–52.
(17) BUA, BUA-Report: Chlorobenzene CAS-No. 108−90−7. *Advisory Committee on Existing Chemicals of Environmental Relevance (BUA)*; Hirzel Verlag, S., Ed.; German Chemical Society, Gesellschaft Deutscher Chemiker: Stuttgart, 1993.
(18) Diez, U.; Rehwagen, M.; Rolle-Kampczyk, U.; Wetzig, H.; Schulz, R.; Richter, M.; Lehmann, I.; Borte, M.; Herbarth, O. Redecoration of apartments promotes obstructive bronchitis in atopy risk infants--results of the LARS Study. *Int. J. Hyg. Environ. Health* **2003**, *206* (3), 173–9.
(19) Lehmann, I.; Thoelke, A.; Weiss, M.; Schlink, U.; Schulz, R.; Diez, U.; Sierig, G.; Emmrich, F.; Jacob, B.; Belcredi, P.; Bolte, G.; Heinrich, J.; Herbarth, O.; Wichmann, H. E.; Borte, M. T cell reactivity in neonates from an East and a West German city--results of the LISA study. *Allergy* **2002**, *57* (2), 129–36.
(20) Lehmann, I.; Rehwagen, M.; Diez, U.; Seiffart, A.; Rolle-Kampczyk, U.; Richter, M.; Wetzig, H.; Borte, M.; Herbarth, O. Enhanced in vivo IgE production and T cell polarization toward the type 2 phenotype in association with indoor exposure to VOC: results of the LARS study. *Int. J. Hyg. Environ. Health* **2001**, *204* (4), 211–21.
(21) Fischader, G.; Roder-Stolinski, C.; Wichmann, G.; Nieber, K.; Lehmann, I. Release of MCP-1 and IL-8 from lung epithelial cells exposed to volatile organic compounds. *Toxicol. In Vitro* **2008**, *22* (2), 359–66.
(22) Sheets, P. L.; Yost, G. S.; Carlson, G. P. Benzene metabolism in human lung cell lines BEAS-2B and A549 and cells overexpressing CYP2F1. *J. Biochem. Mol. Toxicol.* **2004**, *18* (2), 92–9.
(23) Chuang, C. Y.; Chen, T. L.; Chen, R. M. Molecular mechanisms of lipopolysaccharide-caused induction of surfactant protein-A gene expression in human alveolar epithelial A549 cells. *Toxicol. Lett.* **2009**, *191* (2−3), 132–9.
(24) Roder-Stolinski, C.; Fischader, G.; Oostingh, G. J.; Eder, K.; Duschl, A.; Lehmann, I. Chlorobenzene induces the NF-kappa B and p38 MAP kinase pathways in lung epithelial cells. *Inhal. Toxicol.* **2008**, *20* (9), 813–20.
(25) den Besten, C.; Vet, J. J.; Besselink, H. T.; Kiel, G. S.; van Berkel, B. J.; Beems, R.; van Bladeren, P. J. The liver, kidney, and thyroid toxicity of chlorinated benzenes. *Toxicol. Appl. Pharmacol.* **1991**, *111* (1), 69–81.
(26) Feltens, R.; Mogel, I.; Roder-Stolinski, C.; Simon, J. C.; Herberth, G.; Lehmann, I. Chlorobenzene induces oxidative stress in human lung epithelial cells in vitro. *Toxicol. Appl. Pharmacol.* **2009**, .
(27) Wichmann, G.; Muhlenberg, J.; Fischader, G.; Kulla, C.; Rehwagen, M.; Herbarth, O.; Lehmann, I. An experimental model for the determination of immunomodulating effects by volatile compounds. *Toxicol. In Vitro* **2005**, *19* (5), 685–93.
(28) Roder-Stolinski, C.; Fischader, G.; Oostingh, G. J.; Feltens, R.; Kohse, F.; von Bergen, M.; Morbt, N.; Eder, K.; Duschl, A.; Lehmann, I. Styrene induces an inflammatory response in human lung epithelial cells via oxidative stress and NF-kappaB activation. *Toxicol. Appl. Pharmacol.* **2008**, *231* (2), 241–7.
(29) Kroger, M.; Hellmann, J.; Toldo, L.; Gluckmann, M.; von Eiff, B.; Fella, K.; Kramer, P. J. Toxicoproteomics: first experiences in a BMBF-study. *Altex* **2004**, *21* (3), 28–40.
(30) Wetmore, B. A.; Merrick, B. A. Toxicoproteomics: proteomics applied to toxicology and pathology. *Toxicol. Pathol.* **2004**, *32* (6), 619–42.
(31) Marouga, R.; David, S.; Hawkins, E. The development of the DIGE system: 2D fluorescence difference gel analysis technology. *Anal. Bioanal. Chem.* **2005**, *382* (3), 669–78.
(32) Jungblut, P. R.; Holzhutter, H. G.; Apweiler, R.; Schluter, H. The speciation of the proteome. *Chem. Cent. J.* **2008**, *2*, 16.
(33) Morbt, N.; Mogel, I.; Kalkhof, S.; Feltens, R.; Roder-Stolinski, C.; Zheng, J.; Vogt, C.; Lehmann, I.; von Bergen, M. Proteome changes in human bronchoalveolar cells following styrene exposure indicate involvement of oxidative stress in the molecular-response mechanism. *Proteomics* **2009**, *9* (21), 4920–33.
(34) Harvilchuck, J. A.; Pu, X.; Klaunig, J. E.; Carlson, G. P. Indicators of oxidative stress and apoptosis in mouse whole lung and Clara cells following exposure to styrene and its metabolites. *Toxicology* **2009**, *264* (3), 171–8.
(35) Nedelcheva, V.; Gut, I.; Soucek, P.; Frantik, E. Cytochrome P450 catalyzed oxidation of monochlorobenzene, 1,2- and 1,4-dichlorobenzene in rat, mouse, and human liver microsomes. *Chem. Biol. Interact.* **1998**, *115* (1), 53–70.
(36) den Besten, C.; Ellenbroek, M.; van der Ree, M. A.; Rietjens, I. M.; van Bladeren, P. J. The involvement of primary and secondary metabolism in the covalent binding of 1,2- and 1,4-dichlorobenzenes. *Chem. Biol. Interact.* **1992**, *84* (3), 259–75.
(37) Kumagai, S.; Matsunaga, I. Identification of urinary metabolites of human subjects exposed to o-dichlorobenzene. *Int. Arch. Occup. Environ. Health* **1995**, *67* (3), 207–9.
(38) Kumagai, S.; Matsunaga, I. Concentrations of urinary metabolites in workers exposed to monochlorobenzene and variation in the concentration during a workshift. *Occup. Environ. Med.* **1994**, *51* (2), 120–4.
(39) Mangal, D.; Vudathala, D.; Park, J. H.; Lee, S. H.; Penning, T. M.; Blair, I. A. Analysis of 7,8-dihydro-8-oxo-2′-deoxyguanosine in cellular DNA during oxidative stress. *Chem. Res. Toxicol.* **2009**, *22* (5), 788–97.
(40) Georgieva, D.; Risch, M.; Kardas, A.; Buck, F.; von Bergen, M.; Betzel, C. Comparative analysis of the venom proteomes of Vipera ammodytes ammodytes and Vipera ammodytes meridionalis. *J. Proteome Res.* **2008**, *7* (3), 866–86.
(41) Neuhoff, V.; Arold, N.; Taube, D.; Ehrhardt, W. Improved staining of proteins in polyacrylamide gels including isoelectric focusing gels with clear background at nanogram sensitivity using Coomassie Brilliant Blue G-250 and R-250. *Electrophoresis* **1988**, *9* (6), 255–62.
(42) Berth, M.; Moser, F. M.; Kolbe, M.; Bernhardt, J. The state of the art in the analysis of two-dimensional gel electrophoresis images. *Appl. Microbiol. Biotechnol.* **2007**, *76* (6), 1223–43.
(43) Strimmer, K. A unified approach to false discovery rate estimation. *BMC Bioinform.* **2008**, *9*, 303.
(44) Strimmer, K. fdrtool: a versatile R package for estimating local and tail area-based false discovery rates. *Bioinformatics* **2008**, *24* (12), 1461–2.
(45) Jehmlich, N.; Schmidt, F.; Taubert, M.; Seifert, J.; von Bergen, M.; Richnow, H. H.; Vogt, C. Comparison of methods for simultaneous identification of bacterial species and determination of metabolic activity by protein-based stable isotope probing (Protein-SIP) experiments. *Rapid Commun. Mass Spectrom.* **2009**, *23* (12), 1871–8.
(46) Müller, S.; Kohajda, T.; Findeiss, S.; Stadler, P.; Washietl, S.; Kellis, M.; von Bergen, M.; Kalkhof, S. Optimization of parameters for coverage of low molecular weight proteins. *Anal. Bioanal. Chem.* , 1–15.
(47) Santos, P. M.; Roma, V.; Benndorf, D.; von Bergen, M.; Harms, H.; Sa-Correia, I. Mechanistic insights into the global response to phenol in the phenol-biodegrading strain Pseudomonas sp. M1 revealed by quantitative proteomics. *Omics* **2007**, *11* (3), 233–51.
(48) Benndorf, D.; Muller, A.; Bock, K.; Manuwald, O.; Herbarth, O.; von Bergen, M. Identification of spore allergens from the indoor mould Aspergillus versicolor. *Allergy* **2008**, *63* (4), 454–60.
(49) Hammer, O.; Harper, D. A. T.; Ryan, P. D. PAST: Paleontological Statistics Software Package for Education and Data Analysis. *Palaeontologia Electronica* **2001 4**, (1), 9.
(50) Joachimiak, M. P.; Weisman, J. L.; May, B. JColorGrid: software for the visualization of biological measurements. *BMC Bioinform.* **2006**, *7*, 225.
(51) Lehmann, I.; Roder-Stolinski, C.; Nieber, K.; Fischader, G. In vitro models for the assessment of inflammatory and immunomodulatory effects of the volatile organic compound chlorobenzene. *Exp. Toxicol. Pathol.* **2008**, *60* (2−3), 185–93.
(52) Gargas, M. L.; Burgess, R. J.; Voisard, D. E.; Cason, G. H.; Andersen, M. E. Partition coefficients of low-molecular-weight

volatile chemicals in various liquids and tissues. *Toxicol. Appl. Pharmacol.* **1989**, *98* (1), 87–99.
(53) Croute, F.; Poinsot, J.; Gaubin, Y.; Beau, B.; Simon, V.; Murat, J. C.; Soleilhavoup, J. P. Volatile organic compounds cytotoxicity and expression of HSP72, HSP90 and GRP78 stress proteins in cultured human cells. *Biochim. Biophys. Acta* **2002**, *1591* (1−3), 147–55.
(54) Duan, X.; Kelsen, S. G.; Clarkson, A. B., Jr.; Ji, R.; Merali, S. SILAC analysis of oxidative stress-mediated proteins in human pneumocytes: new role for treacle. *Proteomics* , .
(55) Martin, H. J.; Breyer-Pfaff, U.; Wsol, V.; Venz, S.; Block, S.; Maser, E. Purification and characterization of akr1b10 from human liver: role in carbonyl reduction of xenobiotics. *Drug Metab. Dispos.* **2006**, *34* (3), 464–70.
(56) Burczynski, M. E.; Lin, H. K.; Penning, T. M. Isoform-specific induction of a human aldo-keto reductase by polycyclic aromatic hydrocarbons (PAHs), electrophiles, and oxidative stress: implications for the alternative pathway of PAH activation catalyzed by human dihydrodiol dehydrogenase. *Cancer Res.* **1999**, *59* (3), 607–14.
(57) Penning, T. M.; Drury, J. E. Human aldo-keto reductases: Function, gene regulation, and single nucleotide polymorphisms. *Arch. Biochem. Biophys.* **2007**, *464* (2), 241–50.
(58) Takahashi, O.; Oishi, S.; Yoneyama, M.; Ogata, A.; Kamimura, H. Antiestrogenic effect of paradichlorobenzene in immature mice and rats. *Arch. Toxicol.* **2007**, *81* (7), 505–17.
(59) Ross, D. Metabolic basis of benzene toxicity. *Eur. J. Haematol. Suppl.* **1996**, *60*, 111–8.
(60) Rietjens, I. M.; den Besten, C.; Hanzlik, R. P.; van Bladeren, P. J. Cytochrome P450-catalyzed oxidation of halobenzene derivatives. *Chem. Res. Toxicol.* **1997**, *10* (6), 629–35.
(61) Croute, F.; Beau, B.; Arrabit, C.; Gaubin, Y.; Delmas, F.; Murat, J. C.; Soleilhavoup, J. P. Pattern of stress protein expression in human lung cell-line A549 after short- or long-term exposure to cadmium. *Environ. Health Perspect.* **2000**, *108* (1), 55–60.
(62) Slebos, D. J.; Ryter, S. W.; Choi, A. M. Heme oxygenase-1 and carbon monoxide in pulmonary medicine. *Respir Res.* **2003**, *4*, 7.
(63) Slebos, D. J.; Ryter, S. W.; van der Toorn, M.; Liu, F.; Guo, F.; Baty, C. J.; Karlsson, J. M.; Watkins, S. C.; Kim, H. P.; Wang, X.; Lee, J. S.; Postma, D. S.; Kauffman, H. F.; Choi, A. M. Mitochondrial localization and function of heme oxygenase-1 in cigarette smoke-induced cell death. *Am. J. Respir. Cell Mol. Biol.* **2007**, *36* (4), 409–17.
(64) Singh, H.; Ashley, R. H. Redox regulation of CLIC1 by cysteine residues associated with the putative channel pore. *Biophys. J.* **2006**, *90* (5), 1628–38.
(65) Banki, K.; Hutter, E.; Colombo, E.; Gonchoroff, N. J.; Perl, A. Glutathione levels and sensitivity to apoptosis are regulated by changes in transaldolase expression. *J. Biol. Chem.* **1996**, *271* (51), 32994–3001.
(66) Rho, H. K.; Park, J.; Suh, J. H.; Kim, J. B. Transcriptional regulation of mouse 6-phosphogluconate dehydrogenase by ADD1/SREBP1c. *Biochem. Biophys. Res. Commun.* **2005**, *332* (1), 288–96.
(67) Kozar, R. A.; Weibel, C. J.; Cipolla, J.; Klein, A. J.; Haber, M. M.; Abedin, M. Z.; Trooskin, S. Z. Antioxidant enzymes are induced during recovery from acute lung injury. *Crit. Care Med.* **2000**, *28* (7), 2486–91.
(68) Kubo, E.; Hasanova, N.; Tanaka, Y.; Fatma, N.; Takamura, Y.; Singh, D. P.; Akagi, Y. Protein expression profiling of lens epithelial cells from Prdx6-depleted mice and their vulnerability to UV radiation exposure. *Am. J. Physiol. Cell Physiol.* , *298* (2), C342–54.
(69) Holcik, M.; Gordon, B. W.; Korneluk, R. G. The internal ribosome entry site-mediated translation of antiapoptotic protein XIAP is modulated by the heterogeneous nuclear ribonucleoproteins C1 and C2. *Mol. Cell. Biol.* **2003**, *23* (1), 280–8.
(70) Cheng, E. H.; Sheiko, T. V.; Fisher, J. K.; Craigen, W. J.; Korsmeyer, S. J. VDAC2 inhibits BAK activation and mitochondrial apoptosis. *Science* **2003**, *301* (5632), 513–7.
(71) Kile, B. T.; Panopoulos, A. D.; Stirzaker, R. A.; Hacking, D. F.; Tahtamouni, L. H.; Willson, T. A.; Mielke, L. A.; Henley, K. J.; Zhang, J. G.; Wicks, I. P.; Stevenson, W. S.; Nurden, P.; Watowich, S. S.; Justice, M. J. Mutations in the cofilin partner Aip1/Wdr1 cause autoinflammatory disease and macrothrombocytopenia. *Blood* **2007**, *110* (7), 2371–80.
(72) White, S. R.; Williams, P.; Wojcik, K. R.; Sun, S.; Hiemstra, P. S.; Rabe, K. F.; Dorscheid, D. R. Initiation of apoptosis by actin cytoskeletal derangement in human airway epithelial cells. *Am. J. Respir. Cell Mol. Biol.* **2001**, *24* (3), 282–94.
(73) Gourlay, C. W.; Ayscough, K. R. The actin cytoskeleton: a key regulator of apoptosis and ageing. *Nat. Rev. Mol. Cell Biol.* **2005**, *6* (7), 583–9.
(74) Phillips, A. C.; Vousden, K. H. E2F-1 induced apoptosis. *Apoptosis* **2001**, *6* (3), 173–82.
(75) Wang, S.; Nath, N.; Fusaro, G.; Chellappan, S. Rb and prohibitin target distinct regions of E2F1 for repression and respond to different upstream signals. *Mol. Cell. Biol.* **1999**, *19* (11), 7447–60.
(76) Fusaro, G.; Wang, S.; Chellappan, S. Differential regulation of Rb family proteins and prohibitin during camptothecin-induced apoptosis. *Oncogene* **2002**, *21* (29), 4539–48.
(77) Grisendi, S.; Mecucci, C.; Falini, B.; Pandolfi, P. P. Nucleophosmin and cancer. *Nat. Rev. Cancer* **2006**, *6* (7), 493–505.
(78) Lee, H. Z.; Wu, C. H.; Chang, S. P. Release of nucleophosmin from the nucleus: Involvement in aloe-emodin-induced human lung non small carcinoma cell apoptosis. *Int. J. Cancer* **2005**, *113* (6), 971–6.
(79) Mehlen, P.; Coronas, V.; Ljubic-Thibal, V.; Ducasse, C.; Granger, L.; Jourdan, F.; Arrigo, A. P. Small stress protein Hsp27 accumulation during dopamine-mediated differentiation of rat olfactory neurons counteracts apoptosis. *Cell Death Differ.* **1999**, *6* (3), 227–33.
(80) Pandey, P.; Saleh, A.; Nakazawa, A.; Kumar, S.; Srinivasula, S. M.; Kumar, V.; Weichselbaum, R.; Nalin, C.; Alnemri, E. S.; Kufe, D.; Kharbanda, S. Negative regulation of cytochrome c-mediated oligomerization of Apaf-1 and activation of procaspase-9 by heat shock protein 90. *EMBO J.* **2000**, *19* (16), 4310–22.
(81) Sur, R.; Lyte, P. A.; Southall, M. D. Hsp27 regulates pro-inflammatory mediator release in keratinocytes by modulating NF-kappaB signaling. *J. Invest. Dermatol.* **2008**, *128* (5), 1116–22.
(82) Park, K. J.; Gaynor, R. B.; Kwak, Y. T. Heat shock protein 27 association with the I kappa B kinase complex regulates tumor necrosis factor alpha-induced NF-kappa B activation. *J. Biol. Chem.* **2003**, *278* (37), 35272–8.
(83) Bialik, S.; Berissi, H.; Kimchi, A. A high throughput proteomics screen identifies novel substrates of death-associated protein kinase. *Mol. Cell. Proteomics* **2008**, *7* (6), 1089–98.
(84) Casas, C.; Ribera, J.; Esquerda, J. E. Antibodies against c-Jun N-terminal peptide cross-react with neo-epitopes emerging after caspase-mediated proteolysis during apoptosis. *J. Neurochem.* **2001**, *77* (3), 904–15.
(85) Mourtada-Maarabouni, M.; Kirkham, L.; Farzaneh, F.; Williams, G. T. Functional expression cloning reveals a central role for the receptor for activated protein kinase C 1 (RACK1) in T cell apoptosis. *J. Leukoc. Biol.* **2005**, *78* (2), 503–14.
(86) Bardales, R. H.; Xie, S. S.; Schaefer, R. F.; Hsu, S. M. Apoptosis is a major pathway responsible for the resolution of type II pneumocytes in acute lung injury. *Am. J. Pathol.* **1996**, *149* (3), 845–52.
(87) Debret, R.; El Btaouri, H.; Duca, L.; Rahman, I.; Radke, S.; Haye, B.; Sallenave, J. M.; Antonicelli, F. Annexin A1 processing is associated with caspase-dependent apoptosis in BZR cells. *FEBS Lett.* **2003**, *546* (2−3), 195–202.
(88) Rhee, H. J.; Kim, G. Y.; Huh, J. W.; Kim, S. W.; Na, D. S. Annexin I is a stress protein induced by heat, oxidative stress and a sulfhydryl-reactive agent. *Eur. J. Biochem.* **2000**, *267* (11), 3220–5.
(89) Kondoh, H.; Lleonart, M. E.; Bernard, D.; Gil, J. Protection from oxidative stress by enhanced glycolysis; a possible mechanism of cellular immortalization. *Histol. Histopathol.* **2007**, *22* (1), 85–90.
(90) Lelli, S. M.; San Martin de Viale, L. C.; Mazzetti, M. B. Response of glucose metabolism enzymes in an acute porphyria model. Role of reactive oxygen species. *Toxicology* **2005**, *216* (1), 49–58.
(91) Wang, M.; Xiao, G. G.; Li, N.; Xie, Y.; Loo, J. A.; Nel, A. E. Use of a fluorescent phosphoprotein dye to characterize oxidative stress-induced signaling pathway components in macrophage and epithelial cultures exposed to diesel exhaust particle chemicals. *Electrophoresis* **2005**, *26* (11), 2092–108.
(92) Orsatti, L.; Forte, E.; Tomei, L.; Caterino, M.; Pessi, A.; Talamo, F. 2-D Difference in gel electrophoresis combined with Pro-Q Diamond staining: a successful approach for the identification of kinase/phosphatase targets. *Electrophoresis* **2009**, *30* (14), 2469–76.
(93) Banki, K.; Hutter, E.; Gonchoroff, N. J.; Perl, A. Molecular ordering in HIV-induced apoptosis. Oxidative stress, activation of caspases, and cell survival are regulated by transaldolase. *J. Biol. Chem.* **1998**, *273* (19), 11944–53.

(94) Lachaise, F.; Martin, G.; Drougard, C.; Perl, A.; Vuillaume, M.; Wegnez, M.; Sarasin, A.; Daya-Grosjean, L. Relationship between posttranslational modification of transaldolase and catalase deficiency in UV-sensitive repair-deficient xeroderma pigmentosum fibroblasts and SV40-transformed human cells. *Free Radic. Biol. Med.* **2001**, *30* (12), 1365–73.
(95) Shetty, S. Regulation of urokinase receptor mRNA stability by hnRNP C in lung epithelial cells. *Mol. Cell. Biochem.* **2005**, *272* (1−2), 107–18.
(96) Velusamy, T.; Shetty, P.; Bhandary, Y. P.; Liu, M. C.; Shetty, S.; Posttranscriptional regulation of urokinase receptor expression by heterogeneous nuclear ribonuclear protein, C. *Biochemistry* **2008**, *47* (24), 6508–17.
(97) Jin, X.; Wang, L. S.; Xia, L.; Zheng, Y.; Meng, C.; Yu, Y.; Chen, G. Q.; Fang, N. Y. Hyper-phosphorylation of alpha-enolase in hypertrophied left ventricle of spontaneously hypertensive rat. *Biochem. Biophys. Res. Commun.* **2008**, *371* (4), 804–9.
(98) Jung, H.; Seong, H. A.; Manoharan, R.; Ha, H. Serine-threonine kinase receptor-associated protein inhibits apoptosis signal-regulating kinase 1 function through direct interaction. *J. Biol. Chem.* , *285* (1), 54–70.
(99) Christian, K. J.; Lang, M. A.; Raffalli-Mathieu, F. Interaction of heterogeneous nuclear ribonucleoprotein C1/C2 with a novel cis-regulatory element within p53 mRNA as a response to cytostatic drug treatment. *Mol. Pharmacol.* **2008**, *73* (5), 1558–67.
(100) Stone, J. R.; Maki, J. L.; Collins, T. Basal and hydrogen peroxide stimulated sites of phosphorylation in heterogeneous nuclear ribonucleoprotein C1/C2. *Biochemistry* **2003**, *42* (5), 1301–8.
(101) Rossner, P., Jr.; Svecova, V.; Milcova, A.; Lnenickova, Z.; Solansky, I.; Sram, R. J. Seasonal variability of oxidative stress markers in city bus drivers Part II. Oxidative damage to lipids and proteins. *Mutat. Res.* **2008**, *642* (1−2), 21–7.
(102) Adams, J. M. Ways of dying: multiple pathways to apoptosis. *Genes Dev.* **2003**, *17* (20), 2481–95.
(103) Xiao, G. G.; Wang, M.; Li, N.; Loo, J. A.; Nel, A. E. Use of proteomics to demonstrate a hierarchical oxidative stress response to diesel exhaust particle chemicals in a macrophage cell line. *J. Biol. Chem.* **2003**, *278* (50), 50781–90.
(104) Liu, M. J.; Takahashi, Y.; Wada, T.; He, J.; Gao, J.; Tian, Y.; Li, S.; Xie, W. The aldo-keto reductase Akr1b7 gene is a common transcriptional target of xenobiotic receptors pregnane X receptor and constitutive androstane receptor. *Mol. Pharmacol.* **2009**, *76* (3), 604–11.
(105) Stoilov, I.; Jansson, I.; Sarfarazi, M.; Schenkman, J. B. Roles of cytochrome p450 in development. *Drug Metabol. Drug Interact.* **2001**, *18* (1), 33–55.
(106) Sladek, N. E. Transient induction of increased aldehyde dehydrogenase 3A1 levels in cultured human breast (adeno)carcinoma cell lines via 5′-upstream xenobiotic, and electrophile, responsive elements is, respectively, estrogen receptor-dependent and -independent. *Chem. Biol. Interact.* **2003**, *143* (144), 63–74.

PR1005718